

Pseudo-spin symmetry in nuclei

R.V.Jolos

Joint Institute for Nuclear Research
Dubna

Content

- Introduction. Symmetries of the nuclear mean field.
- Nuclear shell model
- Pseudo-spin symmetry in spherical and deformed nuclei
- Transformation from normal-oscillator to pseudo-oscillator basis
- Origin of the pseudo-spin symmetry
- Identical bands
- Summary

Introduction

The mean—field theory of the nucleonic interaction plays a role of the microscopic reference theory. Several more specific advanced theories can be built after having introduced the single-nucleonic mean field solutions as a basis. It is, therefore, of fundamental importance to the whole field of the nuclear structure physics to discover, examine and use the consequences of the underlying symmetries, even if they are approximate.

Symmetries imply the existence of the characteristic multiplet structures. From the physics point of view, however, the fact that the nuclear single-particle multiplets exist in the realistic spectra is an intriguing result. Indeed, let us recall that the nuclear mean field is a potential corresponding to the averaging of the nucleon—nucleon interactions over many occupied single-nucleonic configurations.

And if at the end it resembles any simple-looking function it is either incidental or a result of a symmetry. At small deformations the geometrical characteristics such as nucleonic probability distribution in space are very different from those at moderate and large deformations.

However, the small energy-spread of the multiplets is nearly independent of the deformation. This result is remarkable. It signifies the existence of the symmetry of the two-body interactions.

Nuclear shell model

The fundament of Nuclear physics is the shell model. Since its discovery the shell model made enormous impact on almost all aspects of Nuclear physics.

The shell model is marvelous creation, especially when we realize it exists in spite of relatively strong nucleon-nucleon forces.

The shell model in its simplest form is a description of protons and neutrons moving independently in the potential well which is a result of the average action of all nucleons on one. So, this potential well is called a nuclear mean field. It is clear that the mean field should be determined selfconsistently and is in fact a selfconsistent mean field.

We now realize that this mean field feature is a characteristic of many complex systems and is relatively independent of the character of the interparticle forces.

In the history of the nuclear shell model there was period of the initial intensive development and then the period when the majority of nuclear physicists thought that the shell model has no relation to nuclear structure.

The renaissance of the nuclear shell model began by the paper of Maria Göppert-Mayer (1948). She presented strong experiment evidence for the reality of magic numbers 2, 8, 20, 28, 50, 82 and 126 (for neutrons). She based her conclusion not only on binding energies but also on isotopic abundance. Her paper drew attention of nuclear physicists to existence of magic numbers in heavy nuclei. Some of them tried to obtain shell closures at 50, 82 and 126.

The paper of M. Göppert-Mayer was published in August 1948. On December of 1948 already two manuscripts were received in Physical Review. Both presented level schemes which reproduce the magic numbers 50 and 82. However, their schemes suggest also shell closure at 18, 32, 60 or have other problems. Thus, the problem of the construction of the mean field potential describing correctly all magic numbers was not solved.

Up to this moment people believe in LS-coupling, i.e. in the scheme where L , L_z , S , S_z are good (conserving) quantum numbers. With this assumption it was difficult to find a level scheme with shell closure at 50, 82 and 126.

In the papers of M. Göppert-Mayer and J.H.D. Jensen et al. (1949) the strong spin-orbit interaction has been introduced

$$-v_{ls} \bar{l} \cdot \bar{s}$$

$$\bar{l} \cdot \bar{s} = \frac{1}{2} [j(j+1) - l(l+1) - \frac{3}{4}]$$

$$= \begin{cases} l & , j = l + \frac{1}{2} \\ -l-1 & , j = l - \frac{1}{2} \end{cases}$$

$$\text{Splitting} : \sim (2l+1)$$

which give rise to the modern level scheme reproducing all magic numbers. This version of the shell model explains angular and magnetic momenta of odd nuclei, electromagnetic transitions and “islands of isomerism” near shell closures where single particle states may have widely different j -values.

The simplest potential which can be used to describe nuclear mean field is a harmonic oscillator potential

$$\frac{1}{2} m \omega^2 r^2$$

And the Schrodinger equation looks as

$$\left(-\frac{\hbar^2}{2m} \Delta + \frac{1}{2} m \omega^2 r^2 \right) \psi = E \psi$$

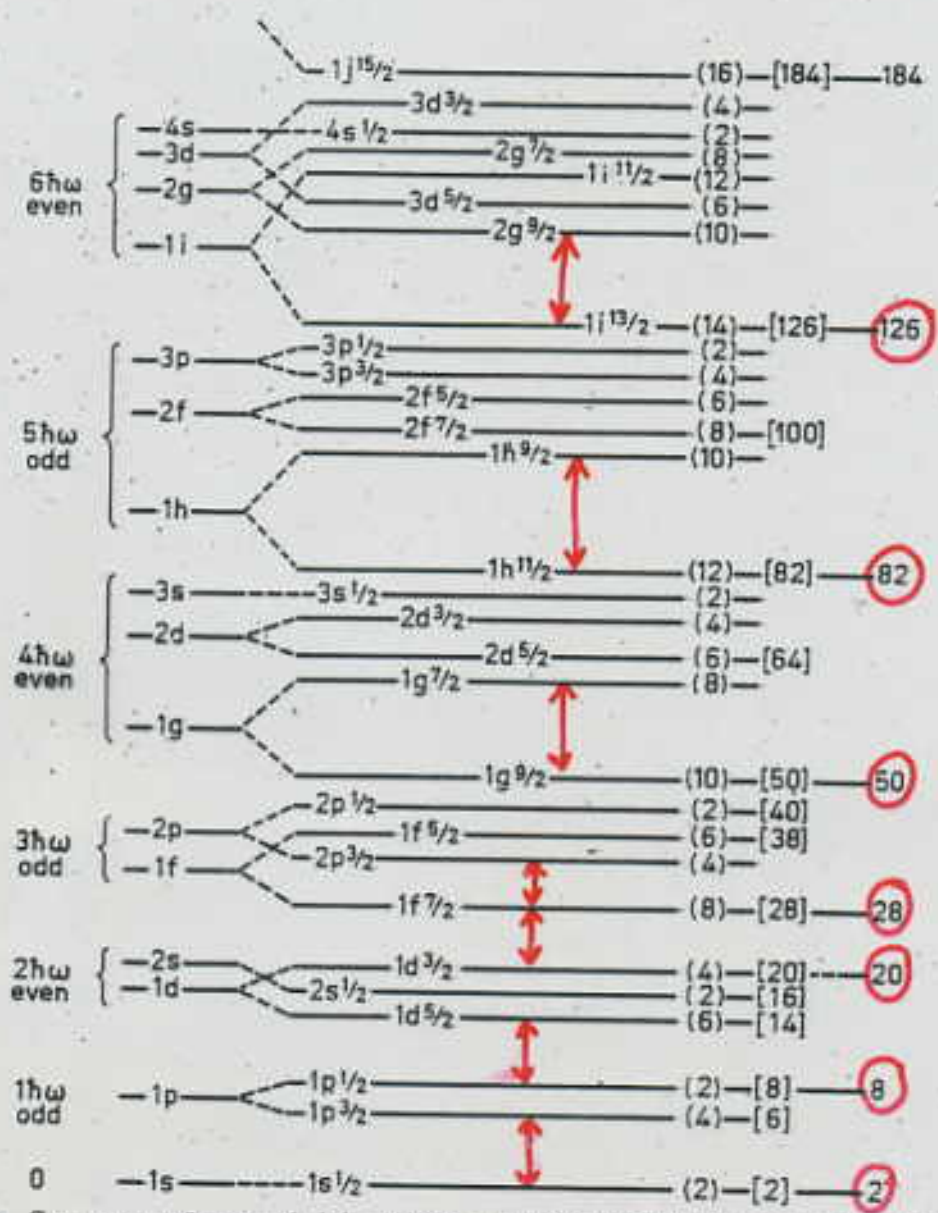


Figure 2-23 Sequence of one-particle orbits. The figure is taken from M. G. Mayer and J. H. D. Jensen, *Elementary Theory of Nuclear Shell Structure*, p. 58, Wiley, New York, 1955.

§ 2-4 AVERAGE NUCLEAR POTENTIAL

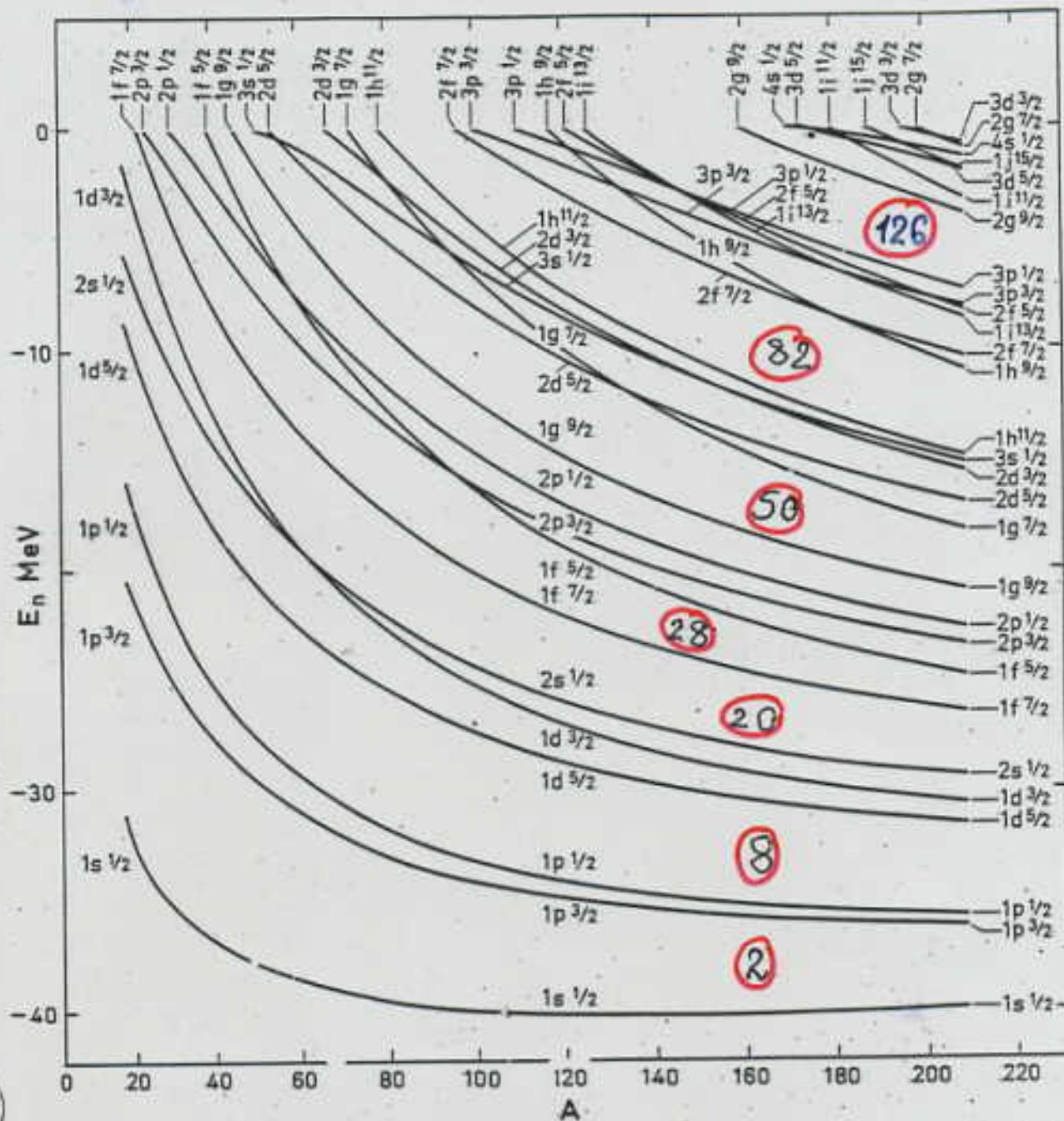


Figure 2-30 Energies of neutron orbits calculated by C. J. Veje (private communication).

Twenty years later, i.e. 35 years ago a quasidegeneracy was observed, at first for spherical nuclei, (Arima, Harvey, ... and Hecht, Adler - 1969):

Single-particle states with $J=1+\frac{1}{2}$ and $J=(1+2)-\frac{1}{2}$ lie very close in energy.

It is convenient to label them as pseudospin doublets with the following quantum numbers

$$\begin{aligned} \tilde{N} &= N-1 \\ \tilde{\ell} &= \begin{cases} \ell_1-1 & , j_1 = \ell_1 - \frac{1}{2} \\ \ell_2+1 & , j_2 = \ell_2 + \frac{1}{2} \end{cases} \\ \tilde{S} &= \frac{1}{2} \end{aligned}$$

This introduction of the pseudospin and pseudoorbital momenta is always possible mathematically

$$a_{n\ell j m}^+ = \sum_{\tilde{m}, \tilde{\sigma}} C_{\tilde{\ell} \tilde{m} \frac{1}{2} \tilde{\sigma}}^{j m} a_{\tilde{N} \tilde{\ell} \tilde{m}, \frac{1}{2} \tilde{\sigma}}^+$$

$$a_{\tilde{N} \tilde{\ell} \tilde{m}, \frac{1}{2} \tilde{\sigma}}^+ = \sum_{j m} C_{\tilde{\ell} \tilde{m} \frac{1}{2} \tilde{\sigma}}^{j m} a_{n\ell j m}^+$$

About two years ago I reexamined these pseudospin doublets, the origin of which remained a mystery, and I discovered that they are a consequence of a relativistic symmetry [6,7]. I discussed this revelation with Dick and he suggested that this symmetry may have some connection with chiral symmetry. In this paper I would like to discuss the progress that has been made in understanding pseudospin symmetry, including an enticing connection with chiral symmetry via QCD sum rules.

2. Pseudospin symmetry

The spherical shell model orbitals that were observed to be quasi-degenerate have non-relativistic quantum numbers $(n_r, \ell, j = \ell + \frac{1}{2})$ and $(n_r - 1, \ell + 2, j = \ell + \frac{3}{2})$ where n_r , ℓ , and j are the single-nucleon radial, orbital, and total angular momentum quantum numbers, respectively [4,5]. This doublet structure is expressed in terms of a "pseudo" orbital angular momentum $\bar{\ell} = \ell + 1$, the average of the orbital angular momentum of the two states in doublet and "pseudo" spin, $\bar{s} = \frac{1}{2}$. For example, $(n_r, s_{1/2}, (n_r - 1)d_{3/2})$ will have $\bar{\ell} = 1$, $(n_r, p_{3/2}, (n_r - 1)f_{7/2})$ will have $\bar{\ell} = 2$, etc. These doublets are almost degenerate with respect to pseudospin, since $j = \bar{\ell} \pm \bar{s}$ for the two states in the doublet; examples are shown in Fig. 1. Pseudospin "symmetry" was shown to exist in deformed nuclei as well [8,9] and has been used to explain features of deformed nuclei, including superdeformation [10] and identical bands [11,12]. However, the origin of pseudospin symmetry remained a mystery and "no deeper understanding of the origin of these (approximate) degeneracies" existed [13]. A few years ago it was shown that relativistic mean field theories gave approximately the correct spin-orbit splitting to produce the pseudospin doublets [14]. In this paper we shall review

Examples of Pseudospin Doublets

$$(n_r, \ell, j; (n_r - 1), \ell + 2, j + 1)$$

$$j = \bar{\ell} \pm \bar{s}, \quad \bar{s} = 1/2;$$

$\bar{\ell}$ pseudo-orbital angular momentum, \bar{s} pseudo-spin

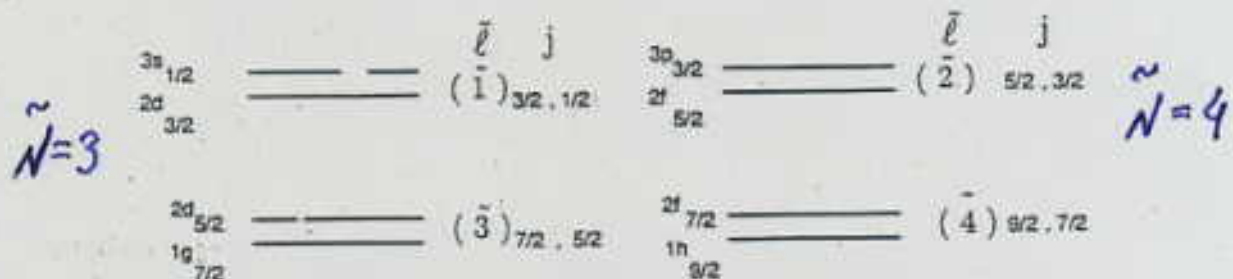


Fig. 1. Examples of pseudospin doublets in the ^{208}Pb region. n_r is the radial quantum number of the state, ℓ is the orbital angular momentum, j the total angular momentum.

The hamiltonian of the single-particle shell model with harmonic oscillator potential with addition of the spin orbit term and the orbit-orbit term has the form

$$| h = h_{osc} + V_{es} \bar{l} \cdot \bar{S} + V_{ee} (\bar{l}^2 - \langle \bar{l}^2 \rangle_{shell})$$

The \bar{l}^2 term is introduced to generate more binding for high- l states within oscillator shell. The last feature occurs naturally in more realistic central potentials like Woods-Saxon,

Splitting generated by $\bar{l} \cdot \bar{S}$ term is large.

In terms of pseudo-spin-orbit operators

$$| h = \tilde{h}_{osc} + (4V_{ee} - V_{es}) \tilde{l} \cdot \tilde{S} + V_{ee} (\tilde{l}^2 - \langle \tilde{l}^2 \rangle_{shell}) + \hbar\omega + V_{ee} - V_{es}$$

It is known empirically that

$$4V_{ee} - V_{es} \approx 0$$

Table

Region	$-V_{es}$	$-V_{\tilde{e}\tilde{s}}$
$50 < Z < 82$	0,127	0,026
$82 < N < 126$	0,127	-0,019
$82 < Z < 126$	0,115	0,035
$126 < N$	0,127	-0,045

Of main importance, however, is to determine if such a scheme helps to classify physically observable states.

The first question is: why pseudo spin-orbital coupling scheme should be seriously considered.

$$- \alpha Q_2 \cdot Q_2$$

$$\langle j_1 j_2 JM | Q_2 \cdot Q_2 | j_1' j_2' JM \rangle = (-1)^{j_1 + j_2' - J} W(j_1 j_2 j_1' j_2'; J 2)$$

$$\times \langle j_1 || Q_2 || j_1' \rangle \langle j_2 || Q_2 || j_2' \rangle$$

$$\langle j || Q_2 || j' \rangle = (-1)^{j' - \frac{1}{2}} \sqrt{\frac{(2j+1)(2j'+1)}{5}} C_{j \frac{1}{2} j' - \frac{1}{2}}^{20}$$

$$\times \int R_{n\ell} R_{n'\ell'} z^4 dz$$

Examples:

$$\int R_{0f} R_{1p} z^4 dz = 3.75$$

$$\int R_{0f}^2 z^4 dz = 4.5$$

Approximation

$$\int R_{ne} R_{n'e'} z^4 dz \rightarrow \text{const}$$

In this case interaction matrix elements depend only on j, j' and we can replace $j = \tilde{l} - \frac{1}{2}$ and $j' = (l-2) + \frac{1}{2}$ orbitals by $\tilde{j} = \tilde{l} + \frac{1}{2}$ and $\tilde{j}' = \tilde{l} - \frac{1}{2}$ without changing any matrix elements of the effective interaction. This replacement means transformation to $\tilde{L}\tilde{S}$ coupling scheme.

Table

$\tilde{l}_1 \tilde{l}_2 \tilde{S} \tilde{L}$	$\tilde{l}_1' \tilde{l}_2' \tilde{S}' \tilde{L}'$	J	SQ ₂ Q ₂	Effective
d ² 0 4	d ² 0 4	4	-0,71	-0,66
d ² 0 4	d ² 1 3	4	0,0	-0,06
d ² 1 3	d ² 1 3	4	1,43	0,44
d ² 1 3	d ² 1 3	3	1,43	0,65
d ² 1 3	d s 1 2	3	0,0	-0,02
d s 1 2	d s 1 2	3	1,75	0,86
d ² 0 2	d ² 0 2	2	0,54	-0,25
d ² 0 2	d ² 1 3	2	0,0	0,10
d ² 0 2	d ² 1 1	2	0,0	0,0
d ² 0 2	d s 0 2	2	2,96	1,0
d ² 0 2	d s 1 2	2	0,0	0,19
d ² 1 3	d ² 1 3	2	1,43	0,50
d ² 1 3	d ² 1 1	2	0,0	0,09
d ² 1 3	d s 0 2	2	0,0	0,42

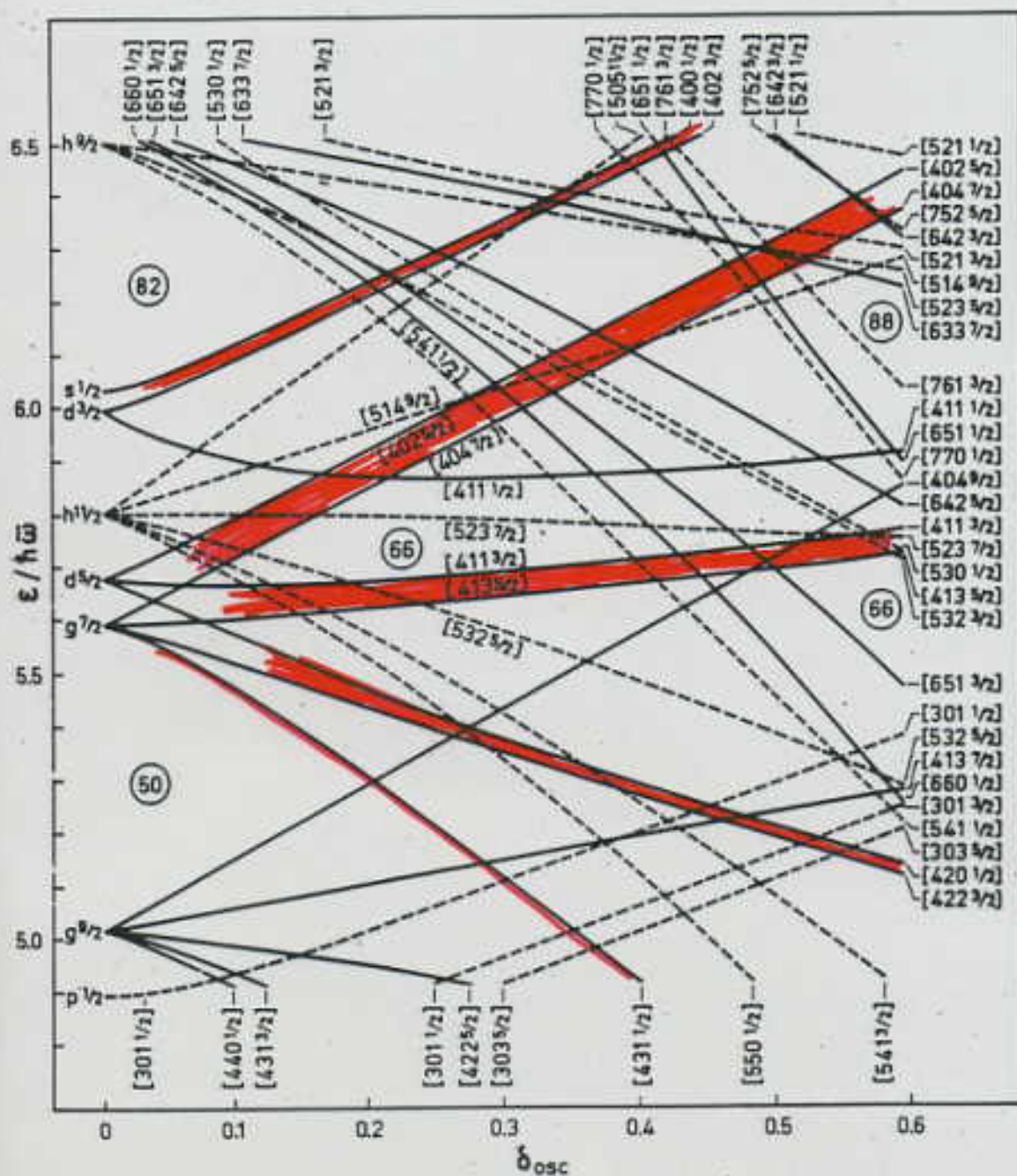


Figure 5-2 Proton orbits in prolate potential ($50 < Z < 82$). The spectra in this and the following figures (Figs. 5-2 to 5-5) are taken from C. Gustafson, I. L. Lamm, B. Nilsson, and S. G. Nilsson, *Arkiv Fysik* 36, 613 (1967). The orbits are labeled by the asymptotic quantum numbers $[Nn_z \Delta\Omega]$. Levels with even and odd parity are drawn with solid and dashed lines, respectively. (Erratum: The orbit $[301 \frac{3}{2}]$ is incorrectly labeled $[301 \frac{1}{2}]$ at bottom of figure.)

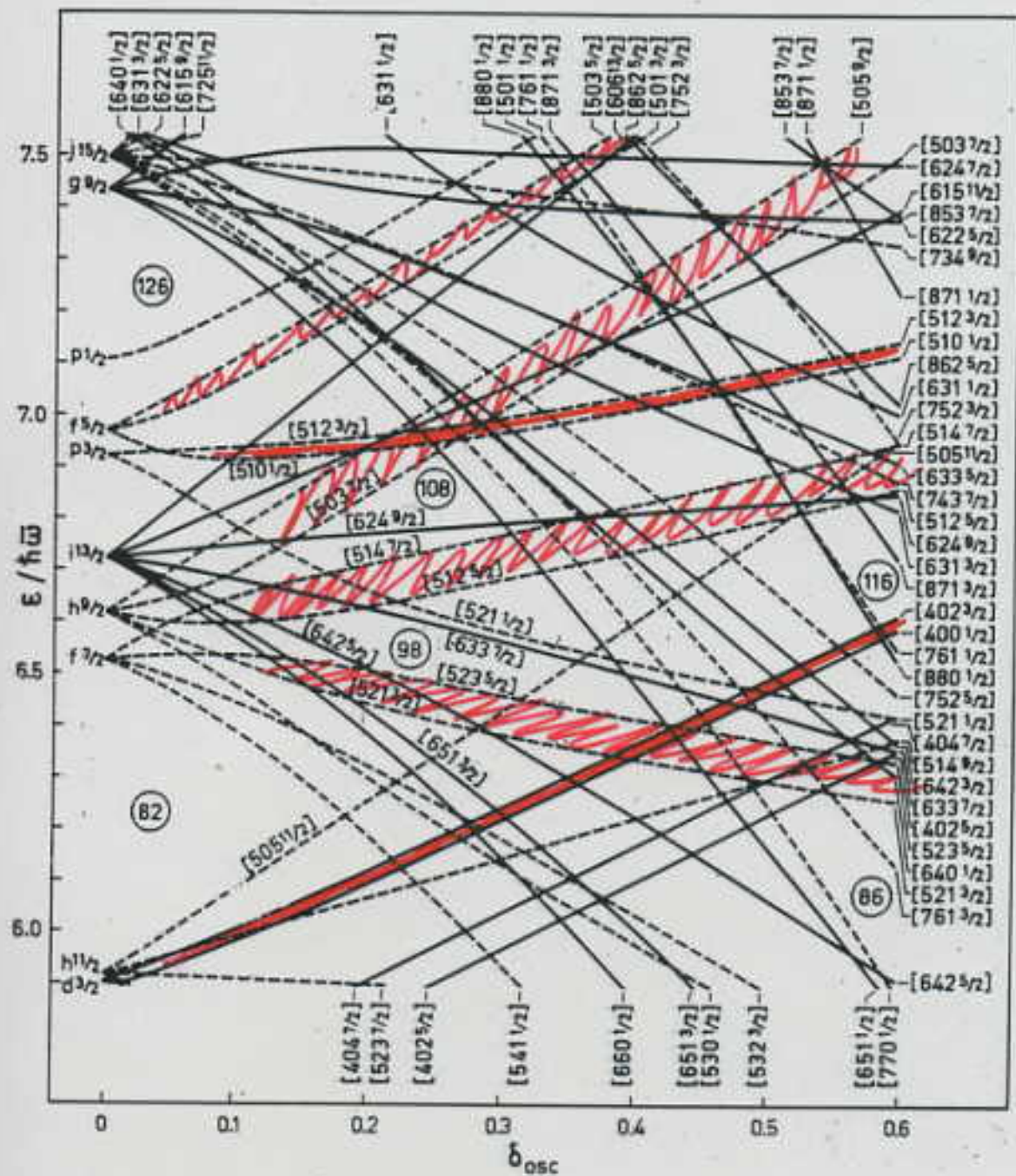
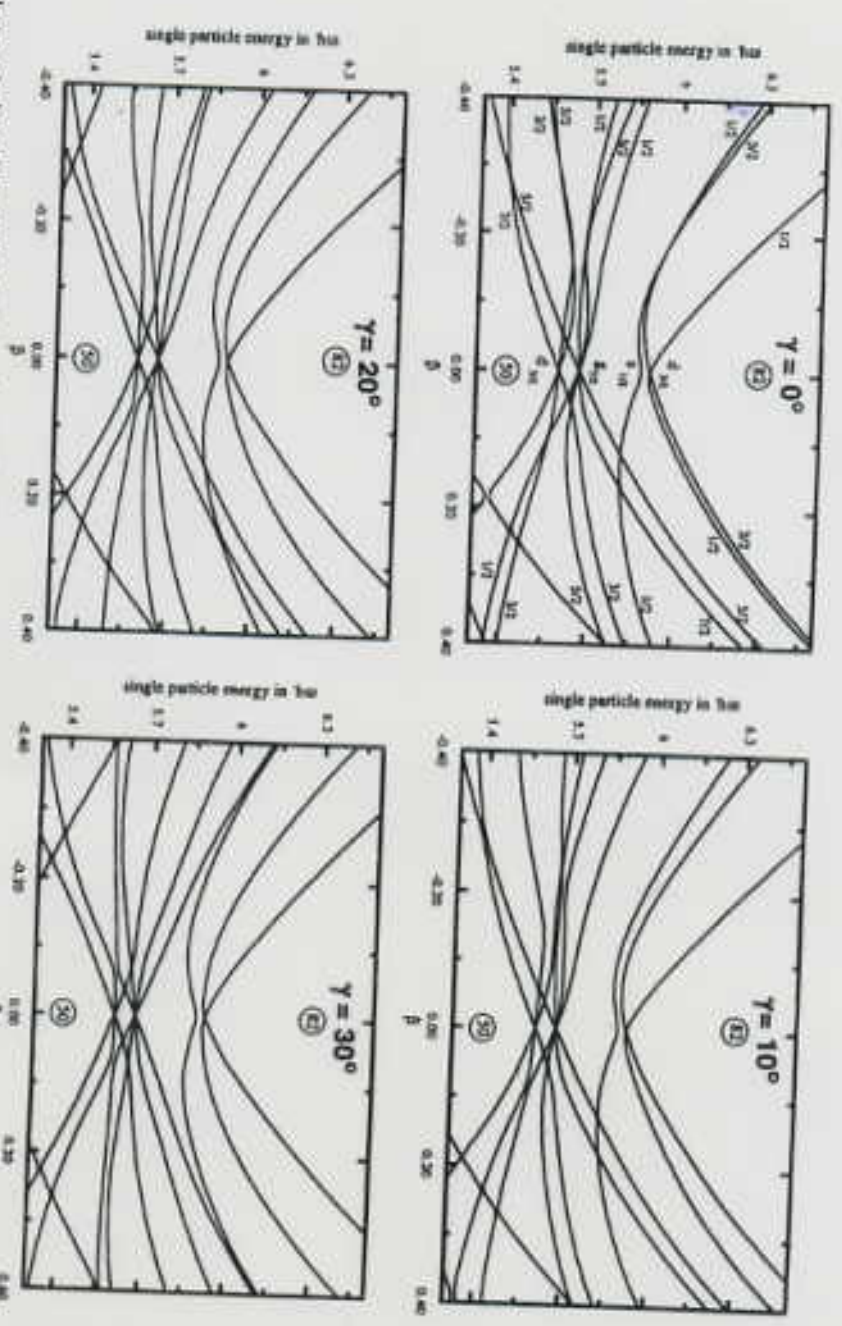


Figure 5-3 Neutron orbits in prolate potential ($82 < N < 126$). See caption to Fig. 5-2.

Fig. 1. Neutron single-particle energies for the $\pi = 4$ normal parity subspaces as a function of β for different triaxial deformations γ . For $\gamma = 0$ the asymptotic states are labeled by $f_1 = l_1 + \frac{1}{2}, \pi_1$ ($f_2 = l_2 + \frac{1}{2}$).



It is seen that splitting of the doublets increase with deviation of γ from $\gamma = 0$. This disappearance of the near degeneracy of the pseudo spin-orbit doublets with increasing triaxiality could be simply a result of the loss of the axial symmetry because $j_z = \Omega$ is no longer a good quantum number. Or it could be more fundamental, i.e. the triaxiality actually destroys the pseudo-spin symmetry.

To determine whether pseudo-spin symmetry is a physically significant concept for nonaxial systems requires a nonspectral measure which can be a correlation coefficient

$$\xi = \frac{\langle\langle (h - \tilde{h})(k - \tilde{k}) \rangle\rangle}{\sqrt{\langle\langle (h - \tilde{h})^2 \rangle\rangle \langle\langle (k - \tilde{k})^2 \rangle\rangle}} = \frac{\langle\langle hk \rangle\rangle - \tilde{h} \cdot \tilde{k}}{\sqrt{\langle\langle (h - \tilde{h})^2 \rangle\rangle \langle\langle (k - \tilde{k})^2 \rangle\rangle}}$$

$\langle\langle \rangle\rangle$ denotes the trace over the model space $\langle\langle k \rangle\rangle = \sum_{i \in n} \langle i | k | i \rangle$
 $\tilde{k} = \langle\langle k \rangle\rangle / d$, d is a dimension of the model space.

Clearly, if $k=h$ $\xi = +1$. If $\xi = 0$ the operators are uncorrelated. Thus, the statement that the pseudo-spin scheme is valid for triaxial nuclei means that the correlation coefficient between $h=h_{\text{nil}}$ and $k=\tilde{l}\cdot\tilde{s}$ must be small. The correlation coefficient can not be small if the spectrum displays large $\tilde{l}\cdot\tilde{s}$ splitting.

The calculated results show that ξ for $\tilde{l}\cdot\tilde{s}$ is much smaller by about a factor of 10 than ξ for $l\cdot s$.

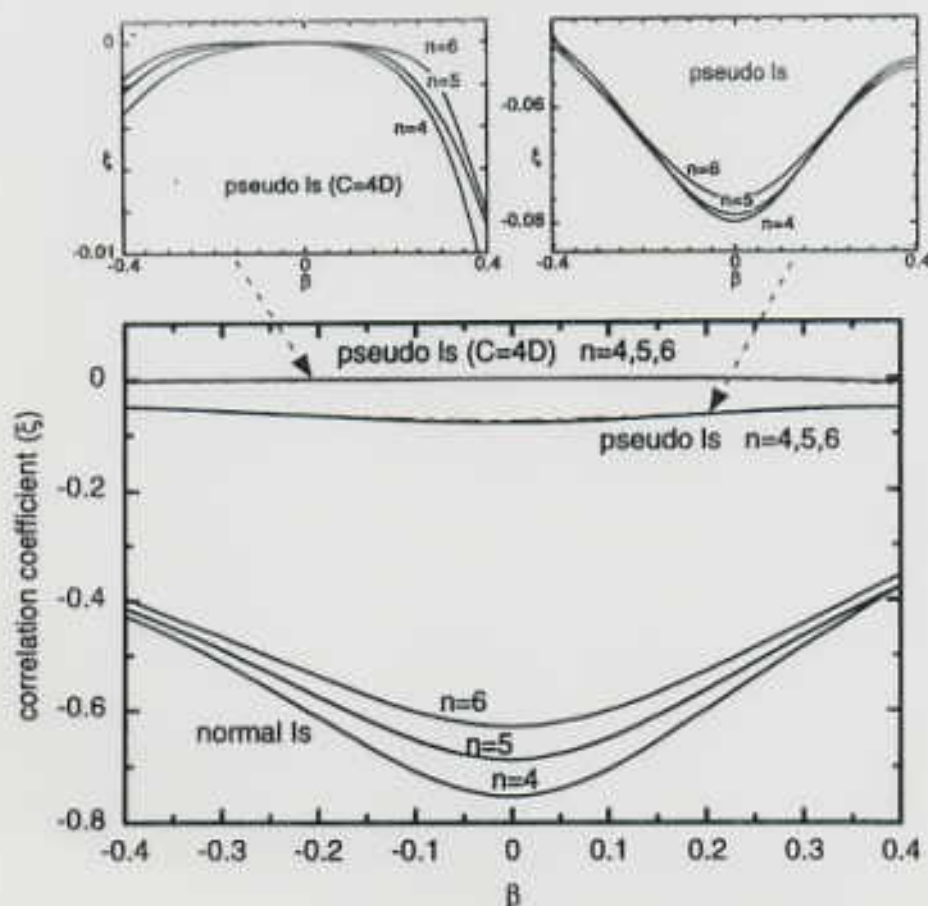


Fig. 2. Correlation coefficients for the $n = 4, 5$ and 6 proton shells; $\gamma = 0$ and $-0.4 \leq \beta \leq 0.4$. To document small differences, the pseudo-spin cases are shown with an expanded y -axis above the main figure.

states of the anisotropic oscillator when there is no spin-orbit ($l \cdot s$) or orbit-orbit (l^2) interaction; in the general case, the deviation of $\langle \hat{n} \rangle$ from n provides a good measure for the mixing generated by the spin-orbit ($l \cdot s$) or orbit-orbit (l^2) interactions.

The generalized Nilsson Hamiltonian, Eq. (7), was also diagonalized in the spherical basis [14] so the eigenstates $|i\rangle$ in Eq. (10) were obtained as

$$|i\rangle = \sum_{n j m_j} c_{i, n j m_j} |n j m_j\rangle, \quad (11)$$

where the $|n j m_j\rangle$ are the eigenfunctions of the isotropic oscillator with the mixing to higher shells explicitly included. In this representation the pseudo transformation (5) can be achieved by simply relabeling the spherical basis states and thus it is a convenient basis to evaluate Eq. (10) when k is an operator defined in the spherical pseudo-spin representation, as $\bar{I} \cdot \bar{s}$ and \bar{I}^2 are.

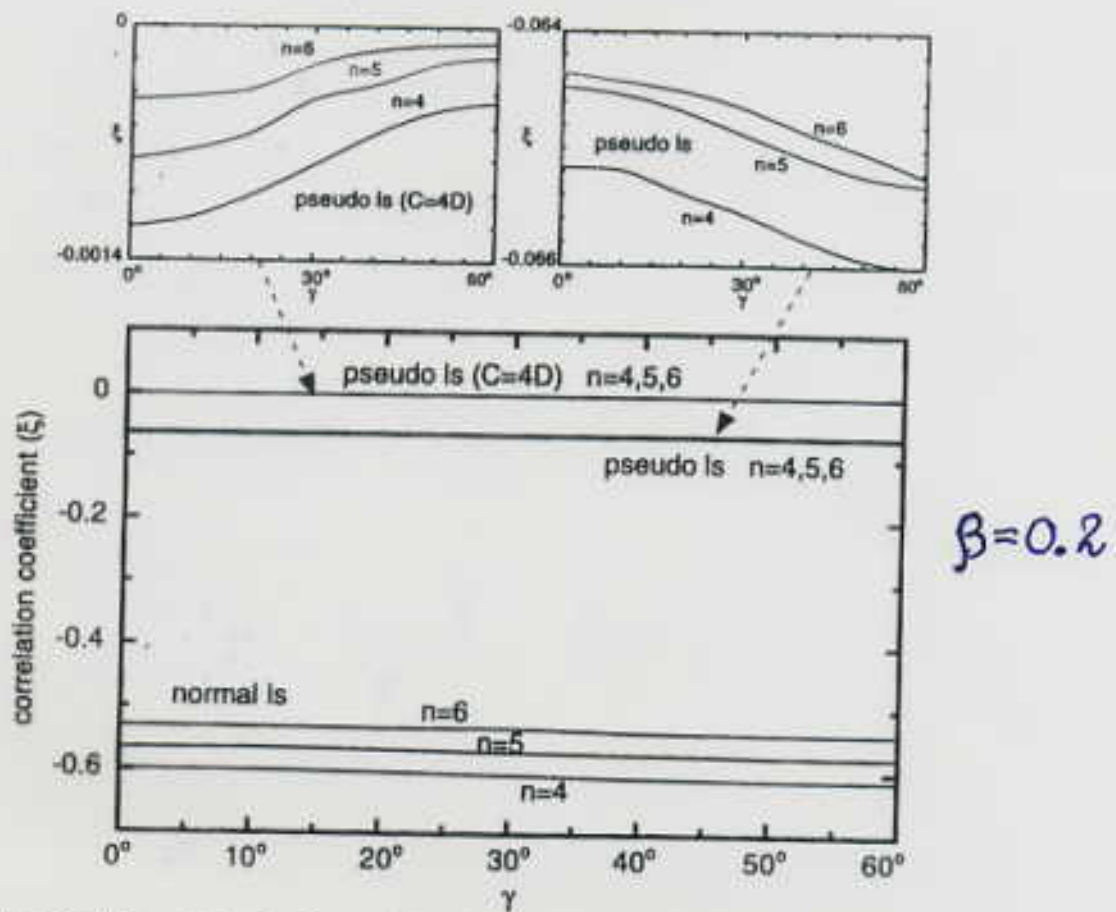


Fig. 3. Correlation coefficients for the $n = 4, 5$ and 6 proton shells; $\beta = 0.2$ and $0^\circ \leq \gamma \leq 60^\circ$ for both the normal and pseudo spin-orbit operators. To document small differences, the pseudo-spin cases are shown with an expanded y -axis in the inserts.

5. Results

The values for C and D of Eq. (7) that were used in the calculations are typical numbers for actinide nuclei [16], namely, $C = 0.1274$ and $D = 0.0382$, or $D = 0.0267$ for protons or neutrons, respectively. To have a scale for comparison, correlation coefficients of the generalized Nilsson Hamiltonian, Eq. (7), with the pseudo ($\vec{l} \cdot \vec{s}$) as well as the normal ($l \cdot s$) spin-orbit operators were calculated. The results are shown in Figs. 2 and 3.

The value of ζ for $4D = C$, which corresponds to exact pseudo-spin symmetry (no $\vec{l} \cdot \vec{s}$ term in the Hamiltonian) in the spherical limit, is very interesting because it provides an independent measure of pseudo-spin splitting induced by the deformation itself. Specifically, for $\beta = 0$, the $\vec{l} \cdot \vec{s}$ term drops out ($4D = C$) of the Hamiltonian, Eq. (2). This yields a correlation coefficient $\zeta = 0$ which, in this case, is a consequence

Transformation
from the normal - oscillator to
the pseudo - oscillator basis

$$H_0 = \frac{1}{2} (\bar{P}^2 + \bar{Q}^2) - \frac{3}{2} \equiv \bar{\eta} \cdot \bar{\xi}$$

$$\bar{\eta} = \frac{1}{\sqrt{2}} (\bar{Q} - i\bar{P}), \quad \bar{\xi} = \frac{1}{\sqrt{2}} (\bar{Q} + i\bar{P})$$

$$\bar{S} = \frac{1}{2} \bar{O}$$

$\bar{\eta}$ - creation operator

$\bar{\xi}$ - annihilation operator

The eigenstates of H_0

$$|N(l, s) j m\rangle = R_{Ne}^{(2)} \sum_{M, G} C_{e\mu}^{jm} \chi_{sG} Y_{e\mu}^{(l, \varphi)}$$

$$s = \frac{1}{2}$$

$$N = 2n + l, \quad l = N, N-2, \dots, 1 \text{ or } 0$$

$$j = l \pm \frac{1}{2}$$

Among the states corresponding to a given N we disregard states with $l = N$, $j = N + \frac{1}{2}$ which in heavy nuclei are shifted down to states of the $(N-1)$ shell (intruder). So, we consider only normal parity states

The normal parity states are mapped into the eigenstates $|\tilde{N}(\tilde{l}, \tilde{s}) \tilde{j} \tilde{m}\rangle$ of the pseudo-oscillator via unitary transformation U

$$U|N(l, s) j m\rangle = |\tilde{N}(\tilde{l}, \tilde{s}) \tilde{j} \tilde{m}\rangle$$

where

$$\tilde{N} = N - 1, \quad \tilde{S} = S, \quad \tilde{j} = j, \quad \tilde{m} = m$$

$$\tilde{l} = l \pm 1 \quad \text{according to } j = l \pm \frac{1}{2}$$

Example:

When $N = 6$ we have orbitals

$$s_{1/2}, d_{3/2}, d_{5/2}, f_{7/2}, f_{5/2}, i_{11/2}, i_{13/2}$$

$i_{13/2}$ is disregarded.

The remaining levels are mapped onto $\tilde{N} = 5$ orbitals

$$\begin{cases} s_{1/2} \rightarrow \tilde{p}_{1/2} \\ d_{3/2} \rightarrow \tilde{p}_{3/2} \end{cases} \quad \begin{cases} d_{5/2} \rightarrow \tilde{f}_{5/2} \\ f_{7/2} \rightarrow \tilde{f}_{7/2} \end{cases}$$

$$\begin{cases} f_{5/2} \rightarrow \tilde{h}_{9/2} \\ i_{11/2} \rightarrow \tilde{h}_{11/2} \end{cases}$$

Let us start with the operator

$$G(\bar{\alpha}, \bar{p}, \bar{S}) = \bar{\xi} \cdot \bar{S}$$

Since $\bar{\xi}$ is annihilation operator

$$(\bar{\xi} \cdot \bar{S}) |N(l, S), j = l + \frac{1}{2}, m\rangle = \frac{1}{2} \sqrt{N-1} |N-1(l+1, S), j = l + \frac{1}{2}, m\rangle$$

$$(\bar{\xi} \cdot \bar{S}) |N(l, S), j = l - \frac{1}{2}, m\rangle = -\frac{1}{2} \sqrt{N+l+1} |N-1(l-1, S), j = l - \frac{1}{2}, m\rangle$$

Apart from some multiplicative factor the normal parity states are transformed as we expected.

So, we must make the operator $\bar{\xi} \cdot \bar{S}$ unitary

$$\begin{aligned} O(\bar{\alpha}, \bar{p}, \bar{S}) &\equiv G^\dagger(\bar{\alpha}, \bar{p}, \bar{S}) G(\bar{\alpha}, \bar{p}, \bar{S}) = (\bar{\eta} \cdot \bar{S})(\bar{\xi} \cdot \bar{S}) \\ &= \frac{1}{4} (\bar{\eta} \cdot \bar{\xi} - 2\bar{L} \cdot \bar{S}) \end{aligned}$$

$$\bar{L} = -i(\bar{\eta} \times \bar{\xi})$$

$$2\bar{L} \cdot \bar{S} = \bar{J}^2 - \bar{L}^2 - \bar{S}^2$$

The operator O is diagonal in the oscillator basis. Then U

$$U = G O^{-\frac{1}{2}} = 2(\bar{\xi} \cdot \bar{S})(\bar{\eta} \cdot \bar{\xi} - 2\bar{L} \cdot \bar{S})^{-\frac{1}{2}}$$

is unitary by construction

Now

$$U \bar{J}^2 U^\dagger = \bar{J}^2$$

$$U \bar{S}^2 U^\dagger = \bar{S}^2$$

$$U \bar{L}^2 U^\dagger = \bar{L}^2 + 4 \bar{L} \cdot \bar{S} + 2$$

$$U \bar{L} \cdot \bar{S} U^\dagger = -\bar{L} \cdot \bar{S} - 1$$

$$U H_0 U^\dagger = H_0 + 1$$

$$H = H_0 - 2k \bar{L} \cdot \bar{S} - k \mu \bar{L}^2$$

$$U H U^\dagger = H_0 + 1 - 2k (2^\mu - 1) \bar{L} \cdot \bar{S} - k \mu \bar{L}^2 \\ - 2k (\mu - 1)$$

The interesting fact is the relation of the transformation from the normal-oscillator to the pseudo-oscillator basis to the superalgebra $Osp(1/2)$.

The operators

$$K_+ = \frac{1}{2} \bar{\eta} \cdot \bar{\eta}$$

$$K_0 = \frac{1}{2} (\bar{\eta} \cdot \bar{\xi} + \frac{3}{2})$$

$$K_- = \frac{1}{2} \bar{\xi} \cdot \bar{\xi}$$

$$F_+ = (\bar{\eta} \cdot \bar{S})$$

$$F_- = (\bar{S} \cdot \bar{\xi})$$

form superalgebra

$$[K_0, K_{\pm}] = \pm K_{\pm}$$

$$[K_+, K_-] = -2K_0$$

$$[K_0, F_{\pm}] = \pm \frac{1}{2} F_{\pm}$$

$$[K_+, F_+] = [K_-, F_-] = 0$$

$$[K_{\pm}, F_{\mp}] = \mp F_{\pm}$$

$$\{F_{\pm}, F_{\pm}\}_+ = K_{\pm}$$

$$\{F_+, F_-\}_+ = K_0$$

The unitary operator U is

$$U = F_- (F_+ F_-)^{-\frac{1}{2}}$$

Many - particle microscopic operator that accomplishes the normal - pseudo transformation

$$U = \prod_{i=1}^A U(\bar{z}_i, \bar{p}_i, \bar{\sigma}_i)$$

$$U = \frac{\bar{\sigma} \cdot \bar{p}}{p}$$

It is the p -helicity operation

In the representation of the plane wave Dirac spinors for nucleon states the p -helicity operation is equivalent to $i\gamma_5 S$ where $\gamma^5 = i\gamma^0\gamma^1\gamma^2\gamma^3$ and $S f(M^*, \bar{p}) = f(-M^*, \bar{p})$. Thus, there is no difference between chiral and helicity transformations in the $M^* \rightarrow 0$ limit. This result indicates on a relation between the pseudo-spin symmetry in heavy nuclei and chiral symmetry of massless hadrons.

Origin of the pseudo-spin symmetry

The origin of the $\bar{1}^2$ term in the single particle harmonic oscillator Hamiltonian is a flatness of the mean field in the interior region as compared with the quadratic form $V(r) = \frac{1}{2} M \omega^2 r^2$. If this spherical potential is replaced by one with an infinite depth the single particle energies are given by

$$E_{nl} = \frac{\hbar^2}{2MR^2} x_{nl}^2$$

where M is the nucleon mass, R is the radius of the well and the x_{nl} are zeroes of the spherical Bessel functions.

Approximately

Table

n	l	x_{nl}/π	$x_{n0}^2 - x_{nl}^2$	$l(l+1)$
4	0	3.000	0.00	0
4	2	2.895	6.11	6
4	4	2.605	21.85	20

The results show that splitting follows an $l(l+1)$ rules. Therefore

$$V_{el} = - \frac{\hbar^2}{2MR^2}$$

Next consider the strength of the spin-orbit coupling. It follows from Dirac equation and using a nonrelativistic reduction that

$$V_{es} = \frac{\hbar^2}{2M} \frac{2}{r} \frac{d}{dr} \left(\frac{1}{1 - B\rho/\rho_0} \right) \bar{l} \cdot \bar{s}$$

In this expression ρ and ρ_0 are respectively the nucleon density at radius \bar{r} and the nuclear matter density. The quantity B is related to the strength of the scalar and vector coupling constants. The spin-orbit strength V_{es} can be obtained from the average of V_{es} over the region inside radius R

$$V_{es} = - \frac{\hbar^2}{2MR^2} \frac{6B}{1-B}$$

Thus,

$$\mu \equiv \frac{2V_{ee}}{V_{es}} = \frac{1-B}{3B}$$

To obtain $\mu = 0.5$ requires $B=0.4$.

In the simplest version of the theory

$$B = \frac{1}{2} (B_s + B_v)$$

With its scalar and vector components given by

$$B_i = g_i^2 \rho_0 / m_i^2 M C^2$$

Where m_i and g_i , respectively denote meson masses and coupling constants. The Nambu-Jona-Lasinio model which starts with massless quarks and generate hadron masses by spontaneous symmetry breaking gives

$$\mu = 0,686$$

Other models give $\mu = 0.447$ (Walecka) and $\mu = 0.635$.

The splitting of the degenerate pairs follows a $\tilde{l}(\tilde{l}+1)$ rule. Empirically,

$$\mu_v = 0.4, \quad \mu_\pi = 0.6.$$

Later J. Ginocchio has shown that pseudo-spin symmetry in nuclei arise from nucleons moving in a relativistic mean field which has an attractive scalar and repulsive vector potential nearly equal in magnitude.

The Dirac equation with external scalar, V_S , and vector, V_V , potentials is given by

$$[c \vec{\alpha} \cdot \vec{p} + \beta (m c^2 + V_S) + V_V] \psi = \mathcal{E} \psi$$

where $\vec{\alpha}$ and β are the usual Dirac matrices. In the case of spherical symmetry scalar and vector potentials depend only on the radial coordinate. In this case the orbital angular momentum is not a conserved quantity in general. Instead a nucleon moving in a spherical relativistic field is labeled by a radial quantum number n_2 , total angular momentum j , its projection m , and $k = -\beta (\vec{\sigma} \cdot \vec{L} + 1)$. The eigenvalues of k are $k = \pm (j + 1/2)$; - for aligned spin and + for unaligned spin.

$$\beta = \begin{pmatrix} \mathbf{I} & 0 \\ 0 & -\mathbf{I} \end{pmatrix}, \quad \alpha^i = \begin{pmatrix} 0 & \sigma_i \\ \sigma_i & 0 \end{pmatrix}$$

- Thus, the quantum number k and the radial quantum number n_2 are sufficient to label orbitals. The spherically symmetric Dirac wave function can be written in terms of upper and lower components

$$\psi_{k>0, m} = (g_k [Y_l \chi]_m^{j=l-\frac{1}{2}}, i f_k [Y_{l-1} \chi]_m^{j=l-\frac{1}{2}})$$

$$\psi_{k<0, m} = (g_k [Y_l \chi]_m^{j=l+\frac{1}{2}}, i f_k [Y_{l+1} \chi]_m^{j=l+\frac{1}{2}})$$

where g_k, f_k are the radial wave functions

$$\left[\frac{d}{dr} + \frac{1+k}{r} \right] g_k = (2 - E - V(r)) f_k \quad (1)$$

$$\left[\frac{d}{dr} + \frac{1-k}{r} \right] f_k = (E + \Delta(r)) g_k \quad (2)$$

where r is the radial coordinate in units of $\hbar c/mc^2$, $V(r) = [V_v(r) - V_s(r)]/mc^2$, and E is the binding energy of the nucleon in units of the free nucleon mass.

$$\Delta(r) = [V_s(r) + V_v(r)] / mc^2.$$

In the limit of equality of the magnitude of the of the vector and scalar potentials, $\Delta(r)=0$, the pseudo-spin is exactly conserved. We solve for g_k in Eq. (2) and substitute into Eq. (1)

$$\left[\frac{d^2}{dx^2} + \frac{2}{x} \frac{d}{dx} - \frac{\tilde{\ell}(\tilde{\ell}+1)}{x^2} + (V(x) - 2 + E) \right] f_k = 0 \quad (3)$$

where $x = \sqrt{E} r$, and

$$\tilde{\ell} = k - 1, \quad k > 0$$

$$\tilde{\ell} = -k, \quad k < 0$$

which agrees with original definition of the pseudo-orbital angular momentum.

The physical significance is revealed: "It is the orbital angular momentum" of the lower component of the Dirac wave function and, in this limit, it is a conserved quantum number.

The Schrodinger Eq.(3) with an attractive potential V depends only on the pseudo-orbital angular momentum \tilde{l} and not on k . Hence the eigenenergies do not depend on k but only on \tilde{l} . Thus, the doublets with the same \tilde{l} but different k will be degenerate producing pseudo-spin symmetry. However, in the limit $\Delta = 0$ there will be no bound Dirac valence states. For small Δ there will be approximate pseudo-spin symmetry, *however, and requisite number of bound Dirac valence states for nuclei.*

Such a near equality of the scalar and vector mean fields has been obtained

- in relativistic field theories with interacting nucleons and mesons;
- in relativistic field theories with nucleons interacting via Skyrme-type interactions.

Probably this result is a general feature of any relativistic model which fits nuclear binding energies.

The energy splitting between states with the same pseudo-orbital angular momentum decreases as the binding energy decreases and as \tilde{l} decreases.

Applying QCD sum rules in nuclear matter, the ratio of the scalar and vector selfenergies were determined to be

$$\frac{V_S}{V_V} \approx - \frac{\sigma_N}{8m_q}, \quad m_q \equiv \frac{1}{2}(m_u + m_d)$$

$$\sigma_N = 45 \pm 10 \text{ MeV}$$

where σ_N is the sigma term which arises from the spontaneous breaking of chiral symmetry. For reasonable values of σ_N and quark masses, this ratio is close to -1 . The implication of these results is that chiral symmetry breaking is responsible for a scalar field being approximately equal in magnitude to the vector field, thereby producing pseudo-spin symmetry.

The Dirac Hamiltonian

$$H = \vec{\alpha} \cdot \vec{P} + \beta (mc^2 + V_s) + V_v$$

is invariant under the $SU(2)$ algebra for two limits: $V_s = V_v$ and $V_s = -V_v$.

The later limit has relevance to understand the origin of pseudo-spin symmetry in nuclei.

The generators of the $SU(2)$ algebra which commute with the Dirac Hamiltonian $[H, \hat{S}_i] = 0$ for the case $V_s = -V_v$ are

$$\hat{S}_i = \frac{\vec{\alpha} \cdot \vec{P} \hat{S}_i \vec{\alpha} \cdot \vec{P}}{P^2} \frac{(1+\beta)}{2} + \hat{S}_i \frac{(1-\beta)}{2}$$

where $\hat{S}_i = \frac{1}{2} \hat{\sigma}_i$

$$\hat{S}_i = \begin{pmatrix} \hat{S}_i & 0 \\ 0 & \hat{S}_i \end{pmatrix}$$

$$\hat{\tilde{S}}_i = U_p \hat{S}_i U_p^\dagger = \frac{2 \vec{\sigma} \cdot \vec{P}}{P^2} P_i - \hat{S}_i$$

$U_p = \frac{\vec{\sigma} \cdot \vec{P}}{P}$ is the momentum-helicity unitary operator, which accomplishes the transformation from the normal to pseudo shell model space.

These pseudo-spin generators have the spin operator \hat{S}_i acting on the lower component of the Dirac wave function which has a consequence that the spatial wave functions for the lower components of the two states in the pseudo-spin

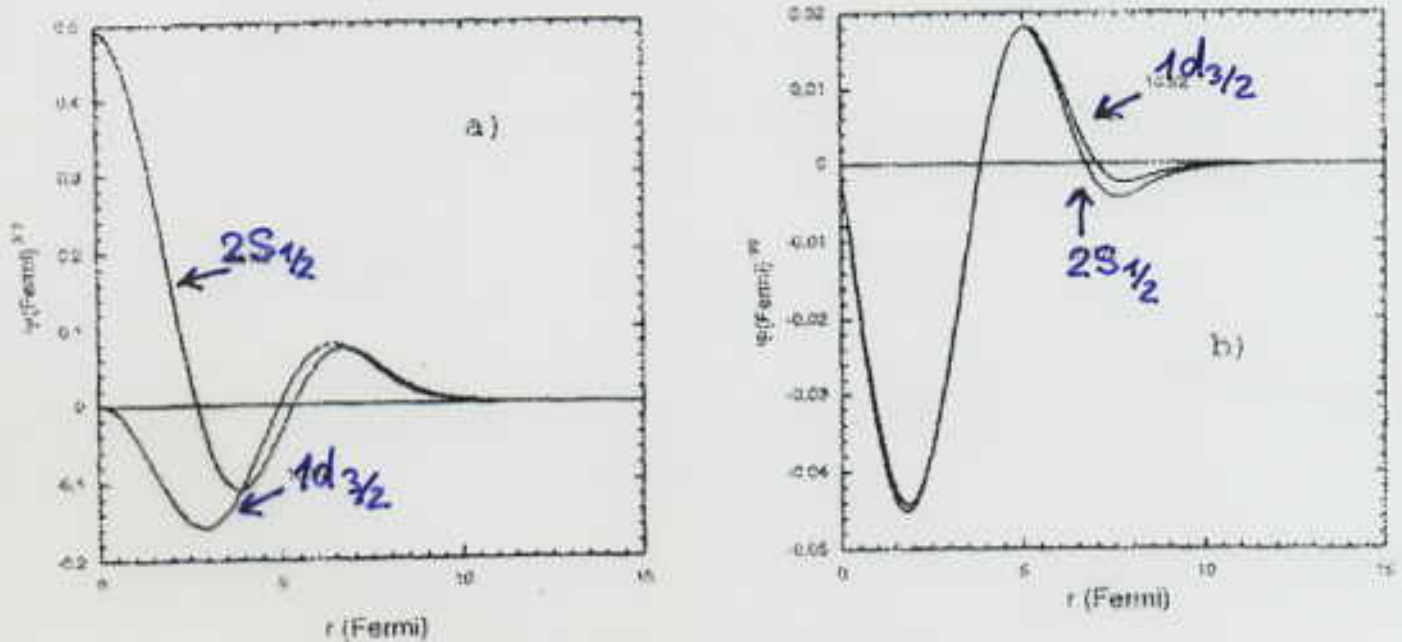
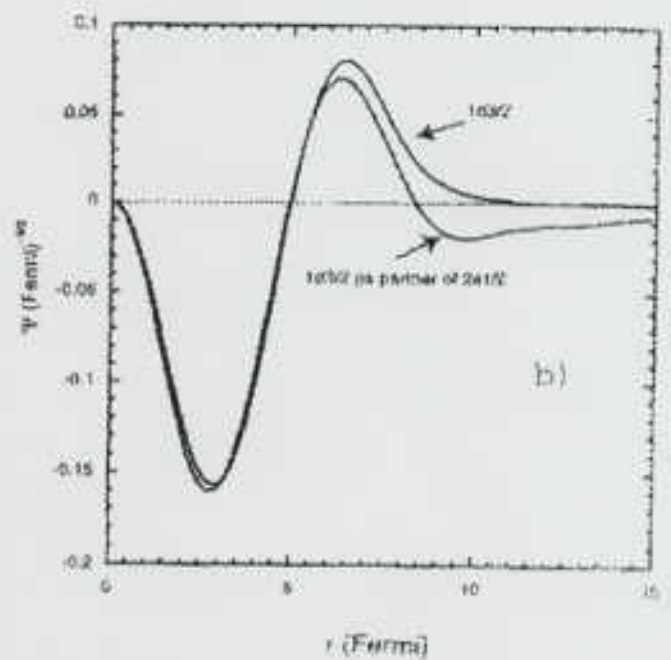
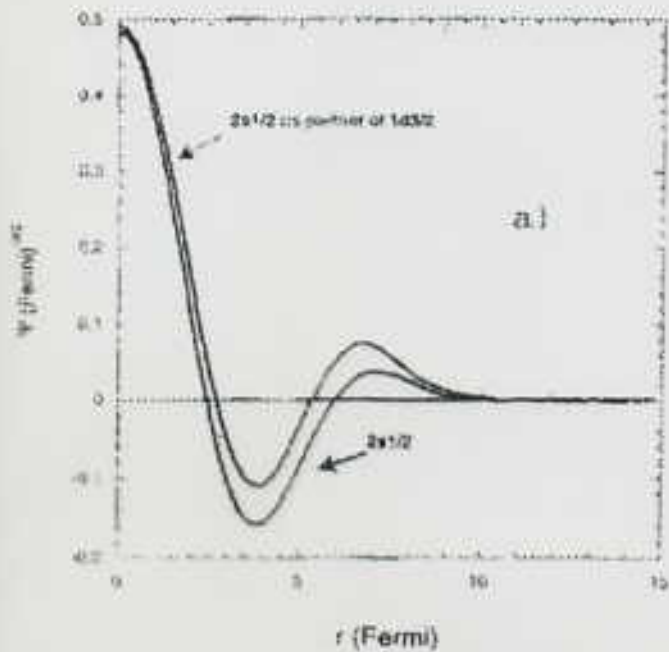


Figure 2. The upper a) and lower components b) of $(2s_{1/2}, 1d_{3/2})$ Dirac eigenfunctions in ^{208}Pb [9].

doublet are identical to within an overall phase.

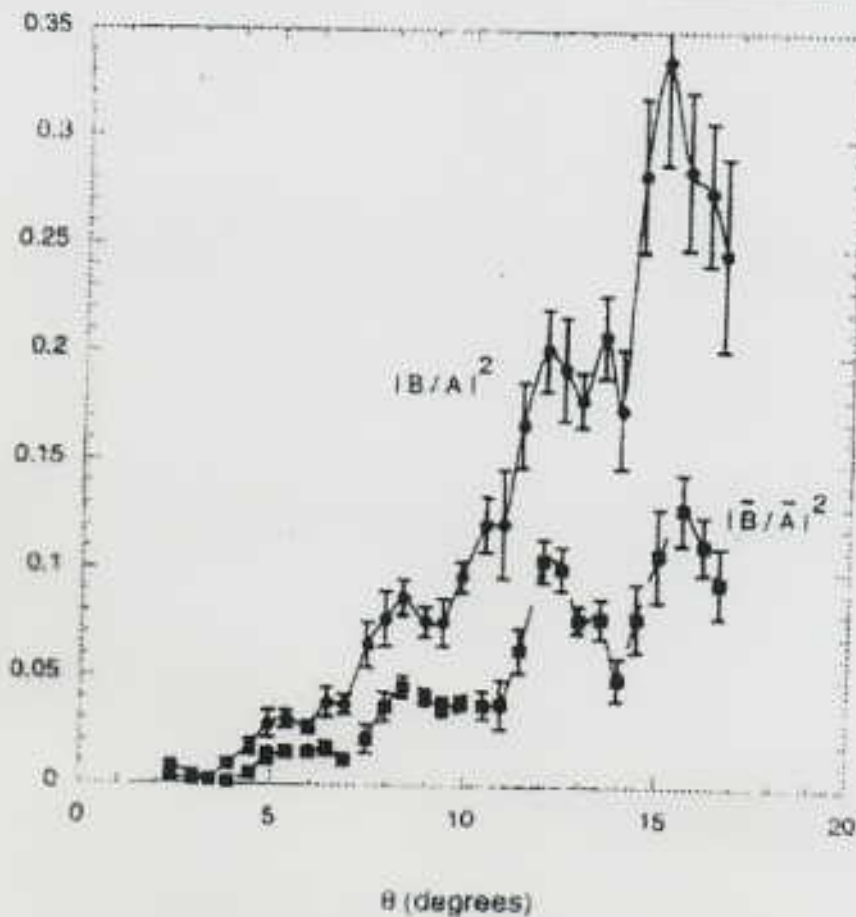
However, the lower components are small. Therefore, the prediction that the lower components are almost identical must be observed in transitions for which upper components are not contribute, like l -forbidden M1 transitions.



Small energy splitting suggests that the pseudo-spin symmetry breaking is small. Is the breaking in the eigenfunctions small as well?

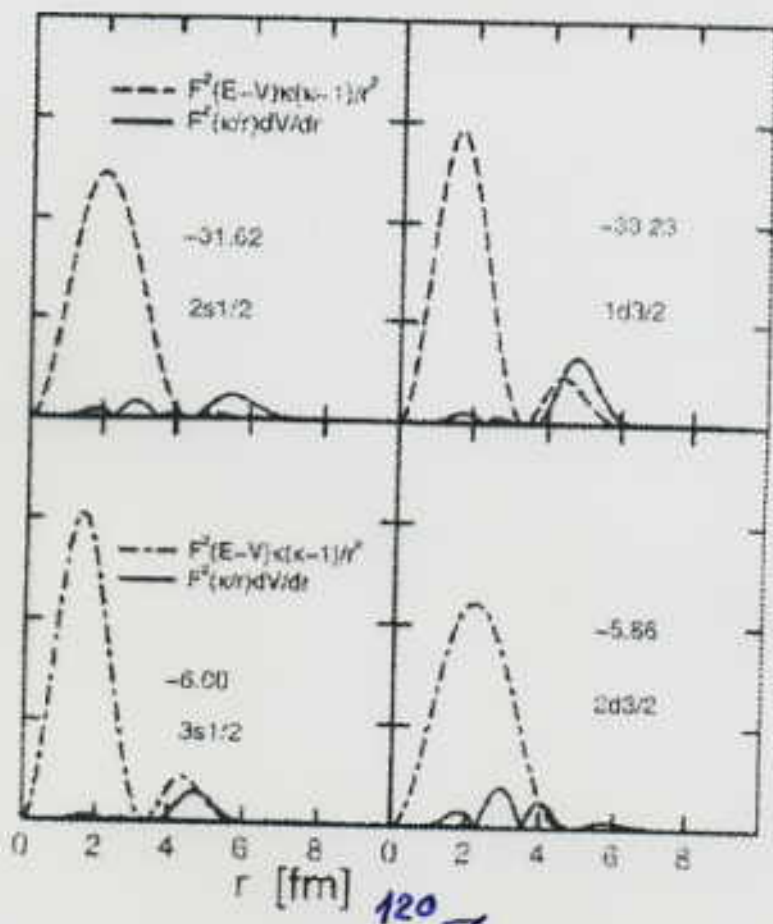
$$f = A(k, \theta) + B(k, \theta) \bar{\sigma} \cdot \bar{n}$$

$$f = \tilde{A}(k, \theta) + \tilde{B}(k, \theta) \tilde{\bar{\sigma}} \cdot \bar{n}$$



The spin $|B/A|^2$ and pseudo-spin $|\tilde{B}/\tilde{A}|^2$ breaking probabilities for 800 MeV proton scattering on ^{208}Pb

In the paper of Meng, Sugawara - Tanabe, Yamaji, Ring and Arima it was demonstrated that the pseudo-spin symmetry is good if the pseudo-spin-orbit interaction is small compare to the effective centrifugal barrier (pseudo).



Comparison of the effective centrifugal barrier and the effective pseudo-spin-orbit potential.

$Z=2$

Table. Experimental (Exp) and relativistic mean field (RMF) pseudo-spin energy splittings for various doublets in ^{208}Pb .

\tilde{T}	doublets	Exp (MeV)	RMF (MeV)
4	$0 h_{9/2} - 1 f_{7/2}$	1.073	2.575
3	$0 g_{7/2} - 1 d_{5/2}$	1.791	4.333
2	$1 f_{5/2} - 2 p_{3/2}$	-0.328	0.697
1	$1 d_{3/2} - 2 s_{1/2}$	0.351	1.247

Table. The binding energies of the pseudo-spin partners in ^{88}Zr and ^{120}Zr .

nlj	^{88}Zr	^{120}Zr	nlj	^{88}Zr	^{120}Zr
$2s_{1/2}$	-31.40	-31.62	$2p_{3/2}$	-16.36	-18.81
$1d_{3/2}$	-33.40	-33.23	$1f_{5/2}$	-18.85	-20.95
$3s_{1/2}$	-1.53	-6.00	$2d_{5/2}$	-3.73	-7.39
$2d_{3/2}$	-1.60	-5.86	$1g_{7/2}$	-4.54	-8.52

The relative weakness of the pseudo-spin-orbit coupling implies that pseudo-orbital angular momenta of the quasiparticles are strongly coupled to the deformation forming, together with the core, a rotating system with angular momentum

$$\bar{\tilde{L}} = \bar{R} + \bar{\tilde{I}}$$

The pseudo-spins are then added to form the total angular momentum

$$\bar{J} = \bar{\tilde{L}} + \bar{\tilde{s}}.$$

Identical bands

The consequence of the pseudo-spin symmetry: the appearance of identical bands. Strong deformation in the pseudo-space part of the many-particle basis gives rise to $\tilde{L} (\tilde{L} + 1)$ rotational sequences for each of the $(2\tilde{S} + 1)$ orientations of the pseudo-spin. A prediction of the theory is that additional, strongly deformed bands should be found.

	(KeV)		(KeV)	
$9\frac{1}{2}^-$	508,22	$11\frac{1}{2}^-$	511,6	\tilde{L} 5
$7\frac{1}{2}^-$	333,26	$9\frac{1}{2}^-$	341,5	4
$5\frac{1}{2}^-$	187,40	$7\frac{1}{2}^-$	190,60	3
$3\frac{1}{2}^-$	74,33	$5\frac{1}{2}^-$	75,04	2
$\frac{1}{2}^-$ $\frac{1}{2} [510]$	0	$\frac{3}{2}^-$ $\frac{3}{2} [512]$	9,746	1

$$\tilde{\Lambda} = 1$$

^{187}Os

EXP	
16 ⁺	3459
14 ⁺	2831
12 ⁺	2241
10 ⁺	1698
8 ⁺	1205
6 ⁺	774
4 ⁺	419
2 ⁺	155
0 ⁺	0
182 Pt	

EXP	
(33/2 ⁻)	3147
(31/2 ⁻)	3067
29/2 ⁻	2521
27/2 ⁻	2465
25/2 ⁻	1960
23/2 ⁻	1906
21/2 ⁻	1445
19/2 ⁻	1397
17/2 ⁻	990
15/2 ⁻	949
13/2 ⁻	604
11/2 ⁻	573
9/2 ⁻	301
7/2 ⁻	278
5/2 ⁻	94
3/2 ⁻	79
1/2 ⁻	0
181 Pt	

CALC.	
(33/2 ⁻)	2874
(31/2 ⁻)	2795
29/2 ⁻	2355
27/2 ⁻	2285
25/2 ⁻	1867
23/2 ⁻	1807
21/2 ⁻	1446
19/2 ⁻	1366
17/2 ⁻	1007
15/2 ⁻	965
13/2 ⁻	649
11/2 ⁻	618
9/2 ⁻	354
7/2 ⁻	332
5/2 ⁻	132
3/2 ⁻	120
1/2 ⁻	0
181 Pt	

EXP		EXP		CALC	
(16) $\overset{+}{\text{---}}$	3209	33/2	3001	33/2	2946
		31/2	2969	31/2	2893
(14) $\overset{+}{\text{---}}$	2598	29/2	2392	29/2	2387
		27/2	2358	27/2	2340
(12) $\overset{+}{\text{---}}$	2020	25/2	1832	25/2	1857
		23/2	1796	23/2	1817
(10) $\overset{+}{\text{---}}$	1486	21/2	1330	21/2	1368
		19/2	1294	19/2	1335
8 $\overset{+}{\text{---}}$	1010	17/2	894	17/2	932
		15/2	862	15/2	905
6 $\overset{+}{\text{---}}$	608	13/2	536	13/2	563
		11/2	508	11/2	542
4 $\overset{+}{\text{---}}$	297	9/2	262	9/2	277
		7/2	242	7/2	262
2 $\overset{+}{\text{---}}$	91	5/2	61	5/2	66
		3/2	69	3/2	78
0 ---	0	1/2	0	1/2	0

174 Hf

173 Hf

173 Hf

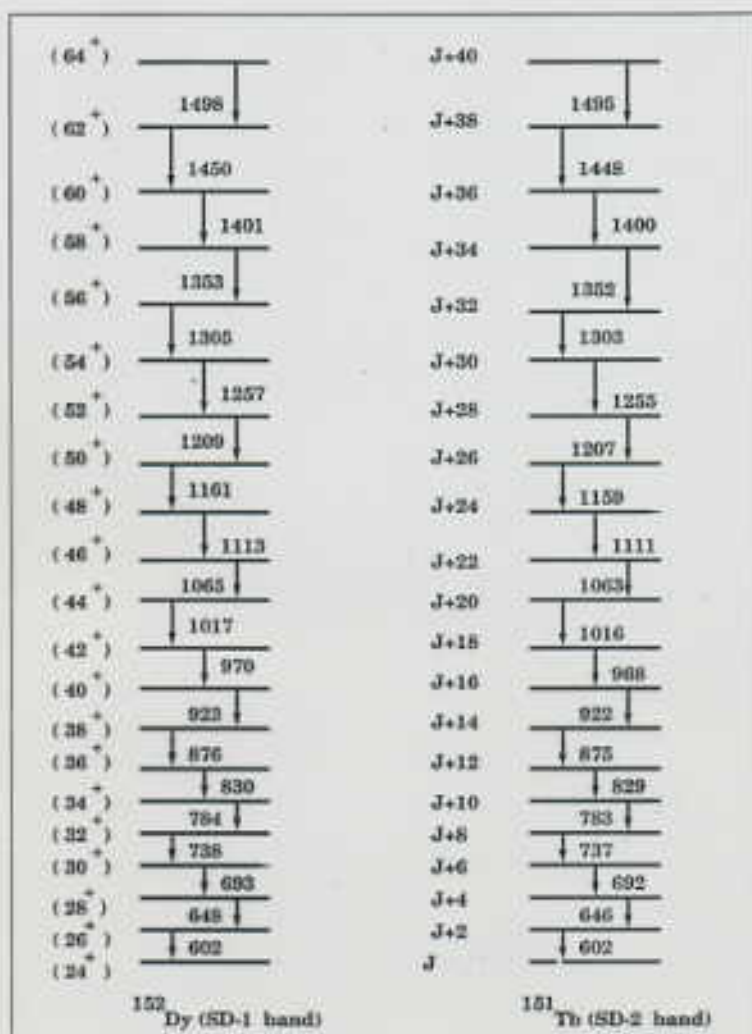


Table. Comparison of the identical bands in ^{151}Tb (yrast) and $^{152}\text{Gd}^*$ (excited).

I	^{151}Tb	I	^{152}Gd
133/2	1380.7	66	1378.0
129/2	1330.0	64	1337.0
125/2	1278.5	62	1277.0
121/2	1228.5	60	1229.0
117/2	1178.9	58	1180.0
113/2	1130.2	56	1130.0
109/2	1082.5	54	1082.0
105/2	1034.9	52	1036.0
101/2	988.7	50	990.0
97/2	942.8	48	944.0
93/2	898.0	46	900.0
89/2	854.0	44	856.0
85/2	811.3	42	813.0
81/2	769.2	40	770.0

Table. Comparison of the identical superdeformed bands in ^{152}Dy (yrast) and ^{151}Tb (excited).

I	^{152}Dy	I	^{151}Tb
59	1353.0	119/2	1353.0
57	1304.7	115/2	1305.0
55	1256.6	111/2	1256.0
53	1208.7	107/2	1207.0
51	1160.8	103/2	1158.0
49	1112.7	99/2	1112.0
47	1064.8	95/2	1063.0
45	1017.0	91/2	1016.0
43	970.0	87/2	970.0
41	923.1	83/2	922.0
39	876.1	79/2	976.0
37	829.2	75/2	828.0
35	783.5	71/2	783.0
33	737.5	67/2	738.0
31	692.2	63/2	692.0
29	647.2	59/2	647.0

Thus,

1. Pseudo-spin symmetry is an approximate relativistic symmetry of the nucleus as demonstrated by experimental data. This symmetry follows from the fact that the vector and scalar potentials of nucleons moving in a relativistic mean field are approximately equal in magnitude and opposite in sign. QCD sum rules in nuclear matter support this conclusion. Such an observation suggests a fundamental reason for pseudo-spin symmetry.
2. The pseudo-spin symmetry improves as the pseudo-orbital angular momentum l decreases and as the binding energy decreases.

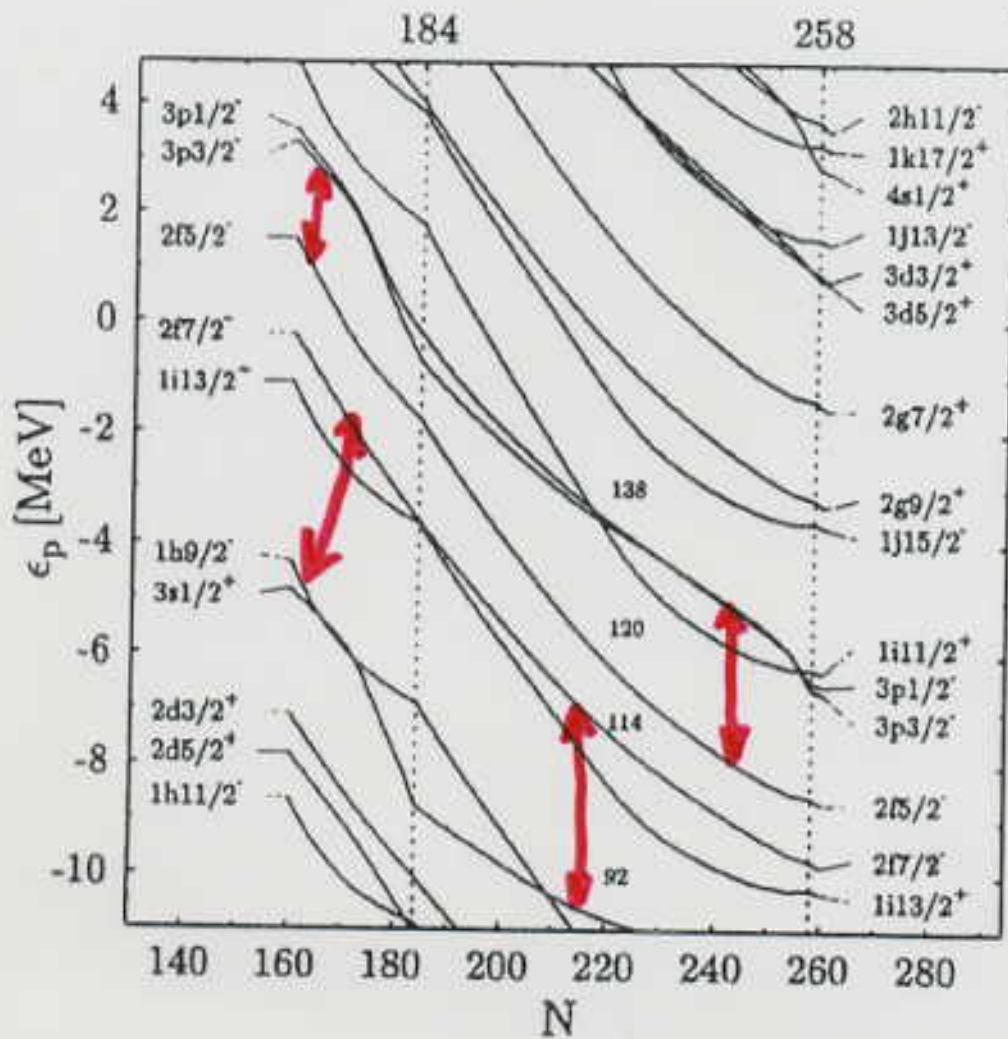
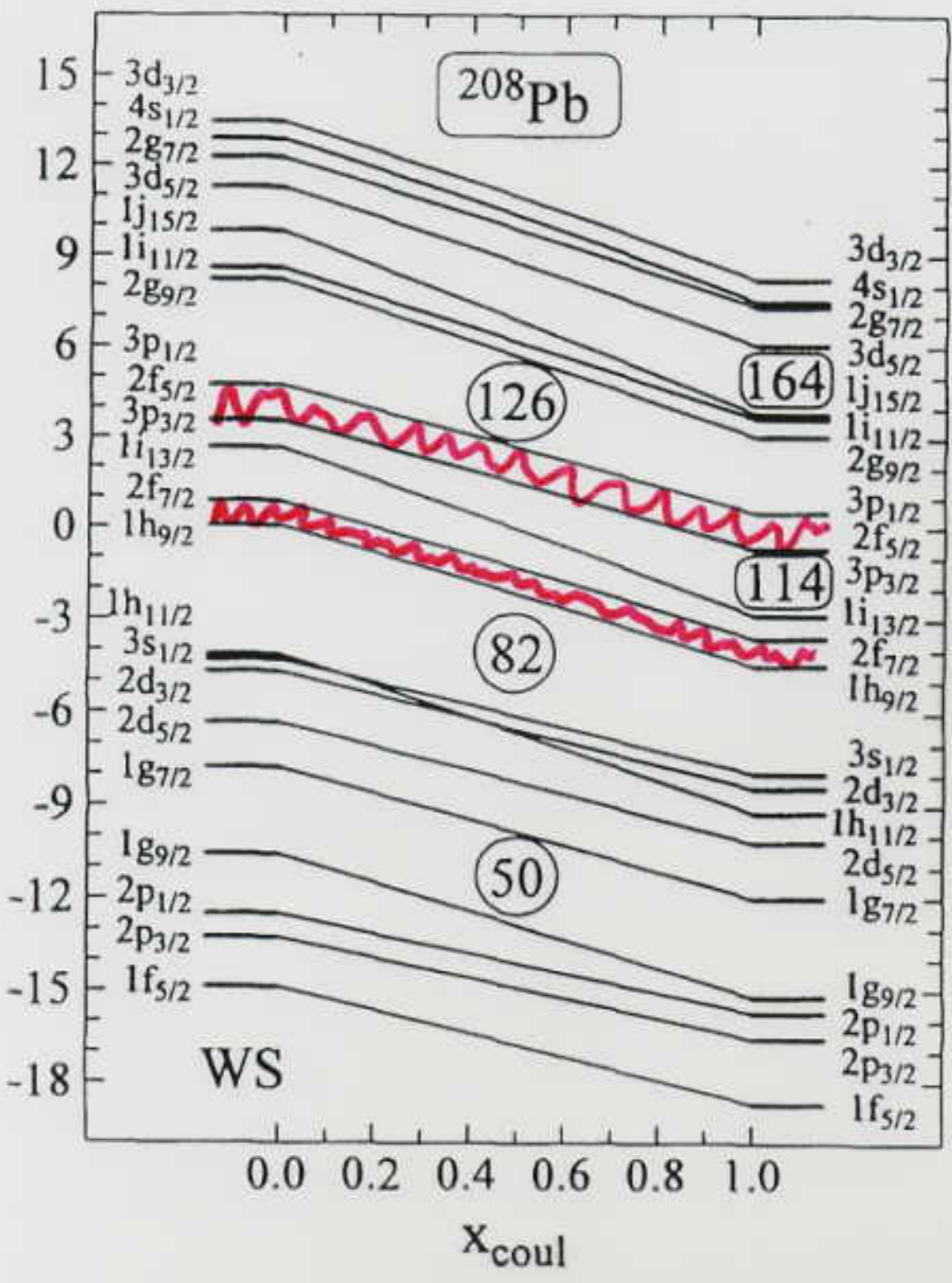


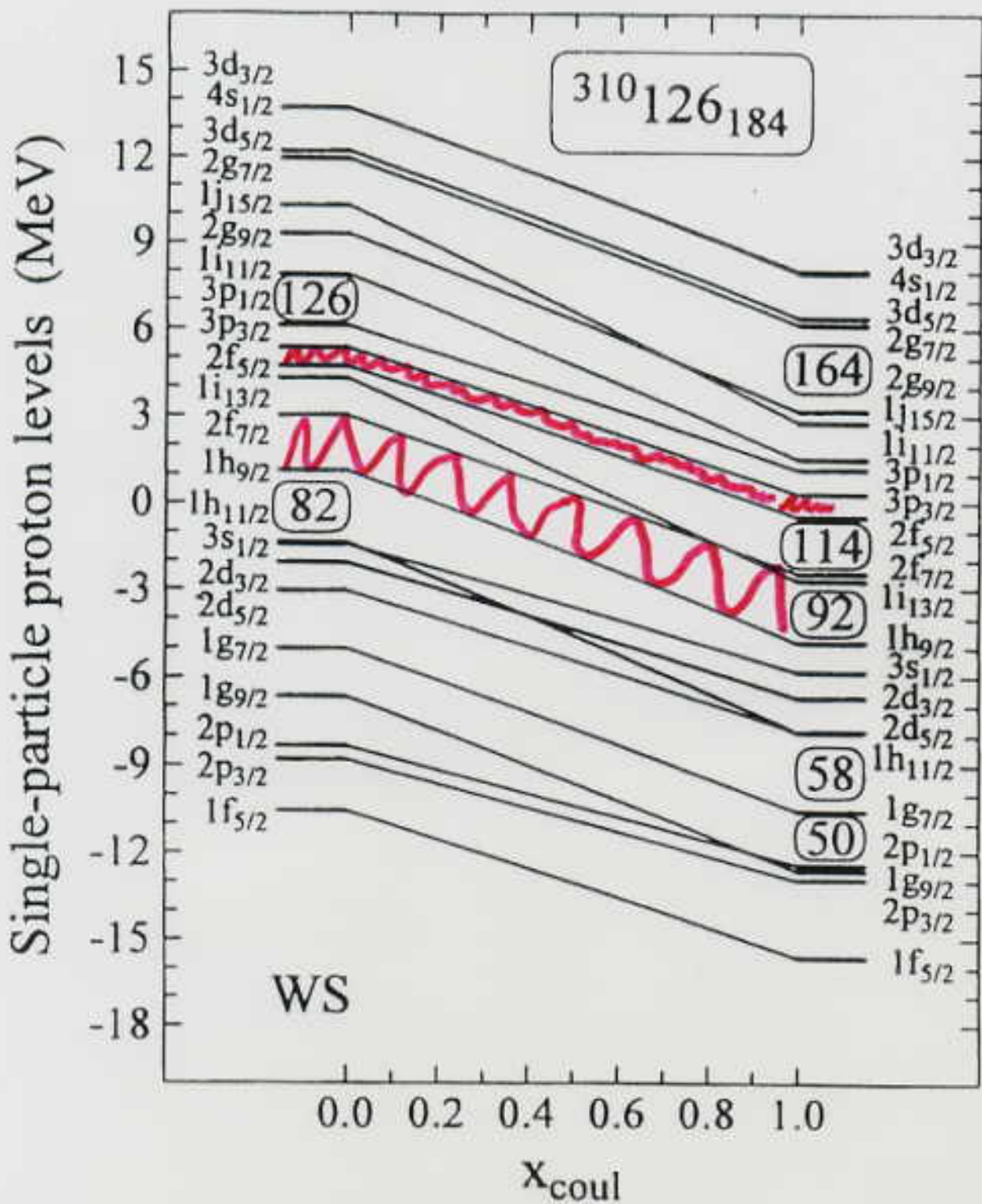
FIG. 2. The single proton levels near the Fermi energy for the isotopes of $Z=120$ versus the neutron number, computed with SkI1. Due to minimal relative changes of the single proton levels the proton gap at $Z=120$ vanishes in the vicinity of $N=184$, the neutron number where the proton shell gap δ_{2p} is lowest, see Fig. 1.

nonrelativistic Skyrme - Hartree - Fock calculations.
 SkI1 forces stems from a recent systematic fit already embracing data from exotic nuclei; it is biased towards an optimal description of normal nuclei including surface properties.

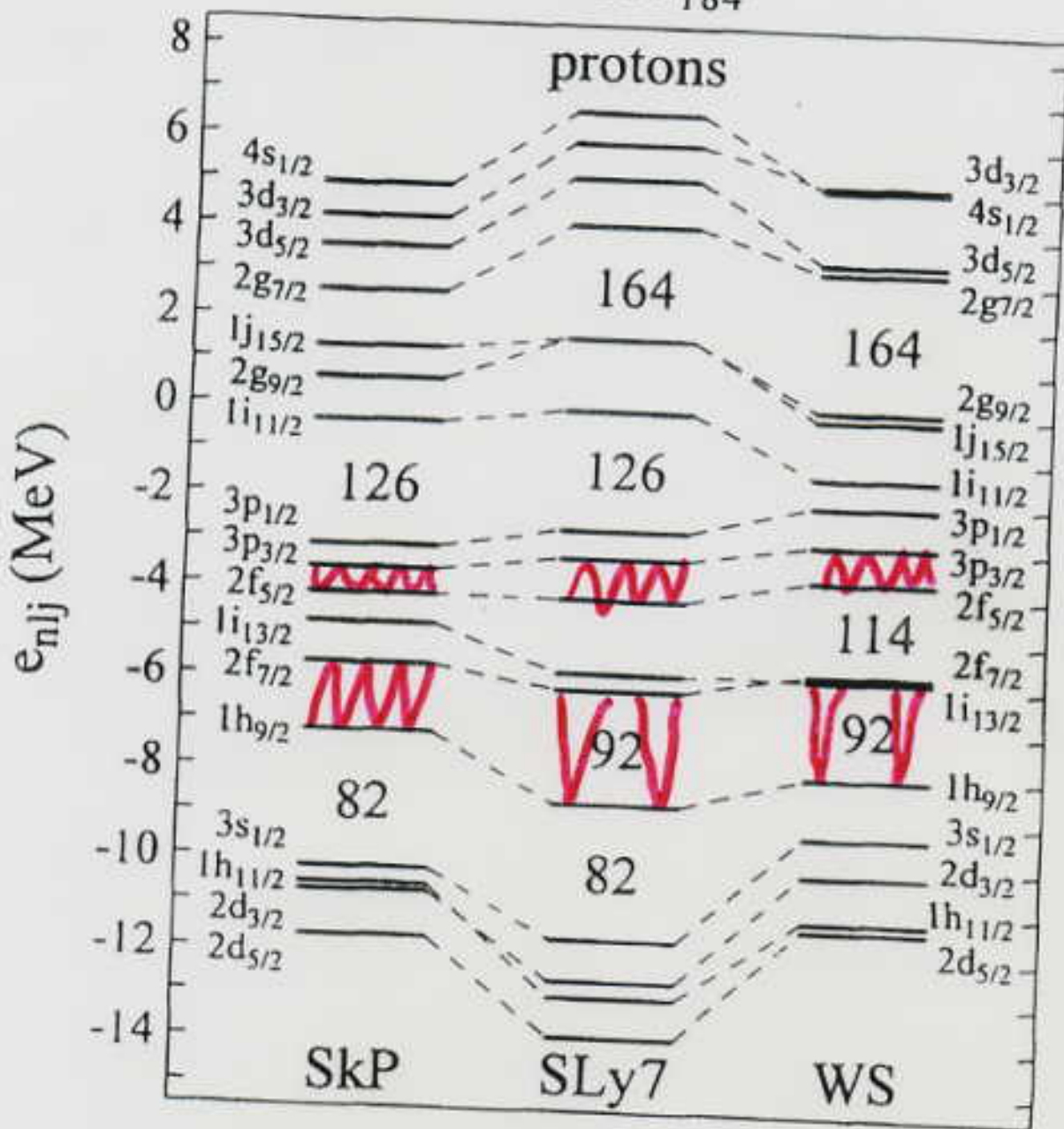
Single-particle proton levels (MeV)



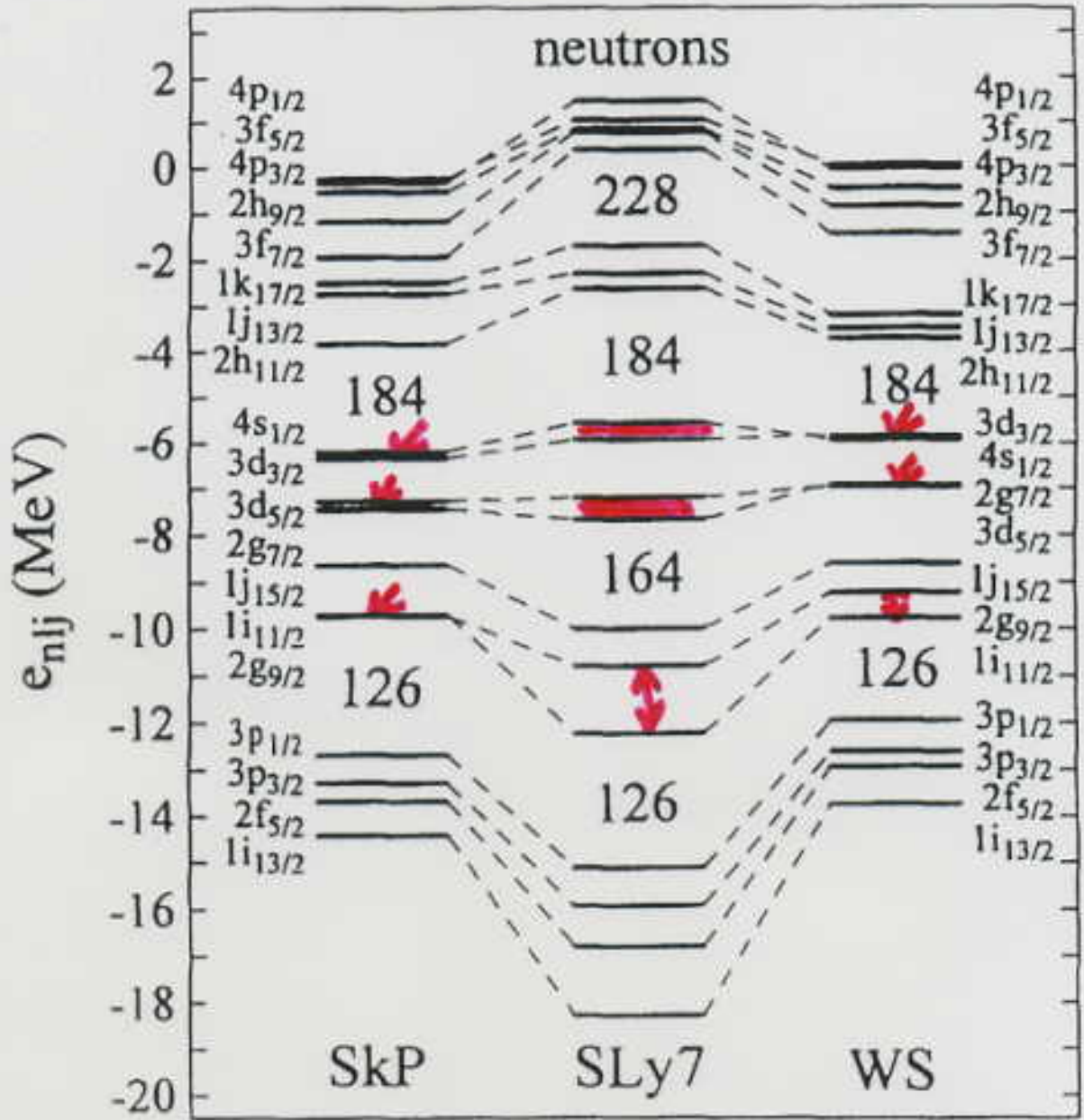
Protons



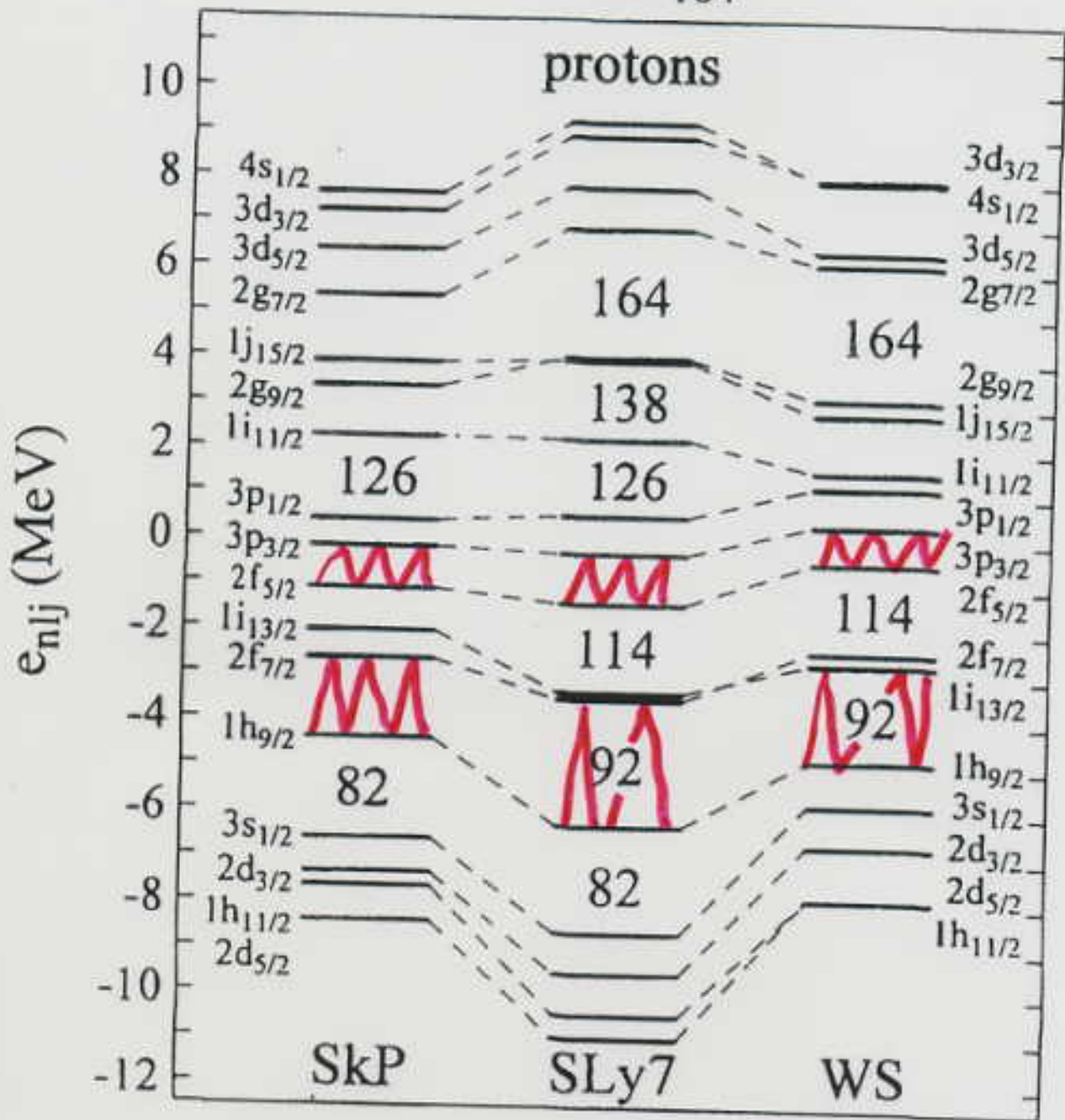
$^{298}_{114}_{184}$



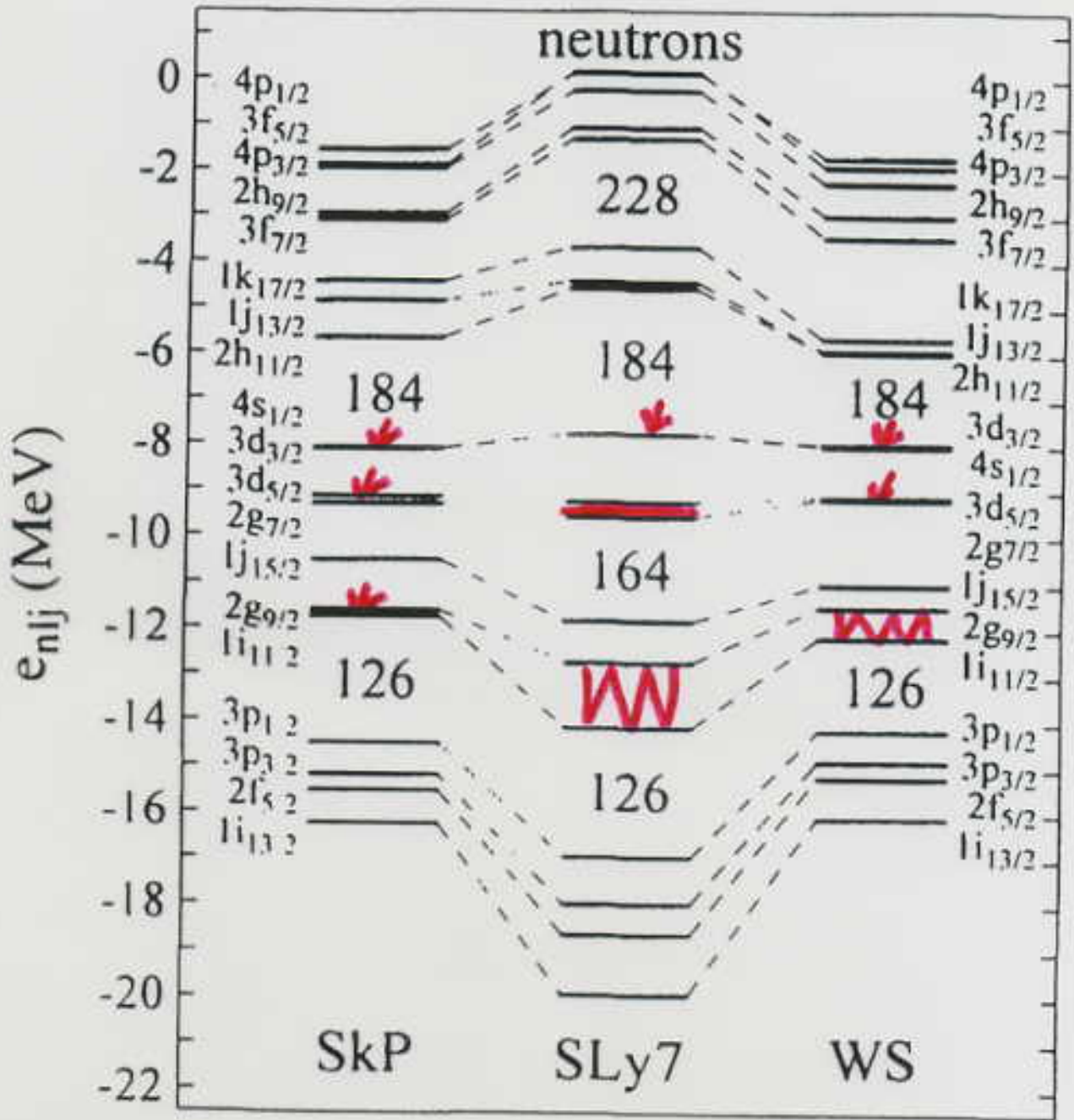
$^{298}_{114}_{184}$



310^{126}_{184}



$^{310}_{126}184$



Summary

1. We have seen that the pseudo-spin symmetry is supported by the experimental data for nuclei belonging to the traditionally investigated regions of the nuclide chart.
2. Pseudo-spin symmetry is justified theoretically.
3. It is interesting will it be confirmed by experimental data for exotic nuclei, for instance, for superheavy nuclei.

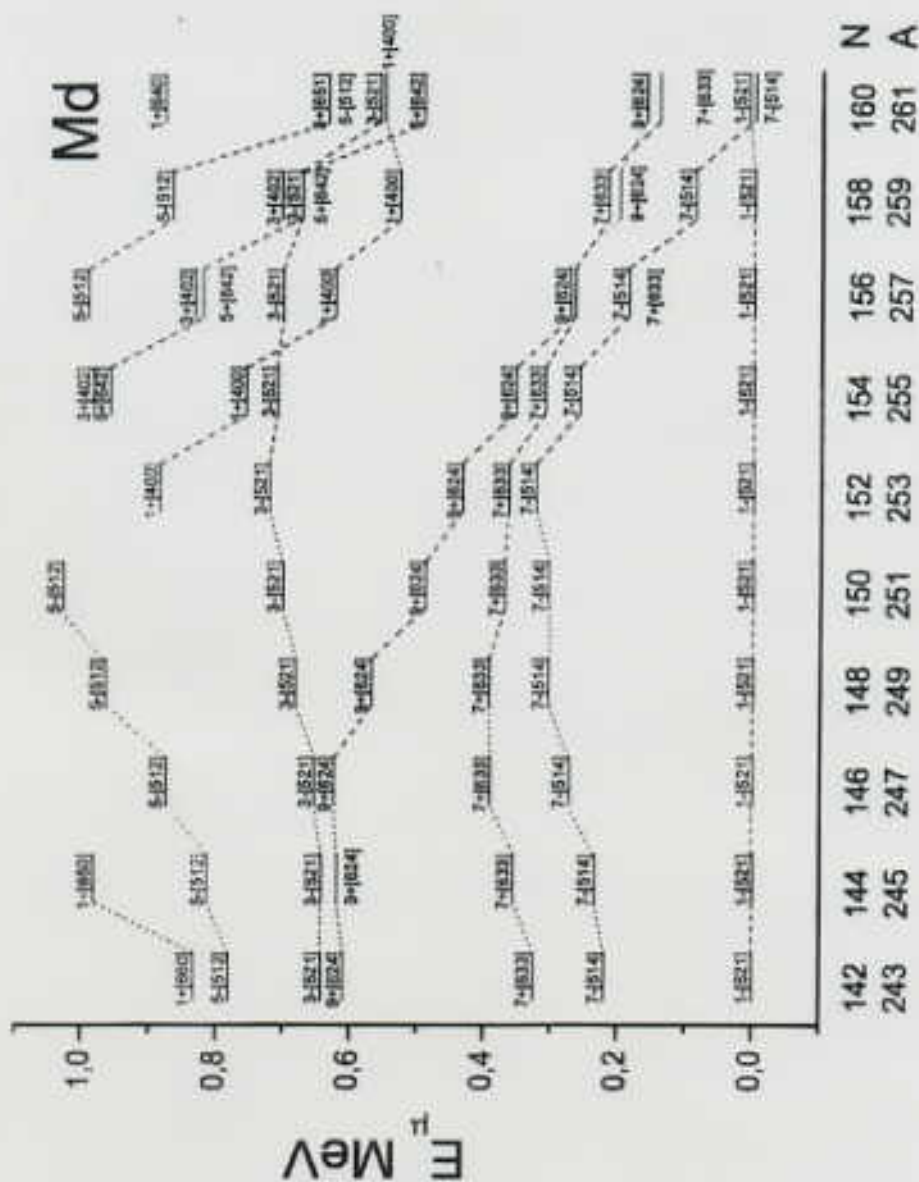


Fig. 7. Same as in Fig. 3, but for mendelevium ($Z = 101$).

$Z = 101$

AP A 723, 354

$\frac{1}{2}^- [521]$ pseudo-spin singlet

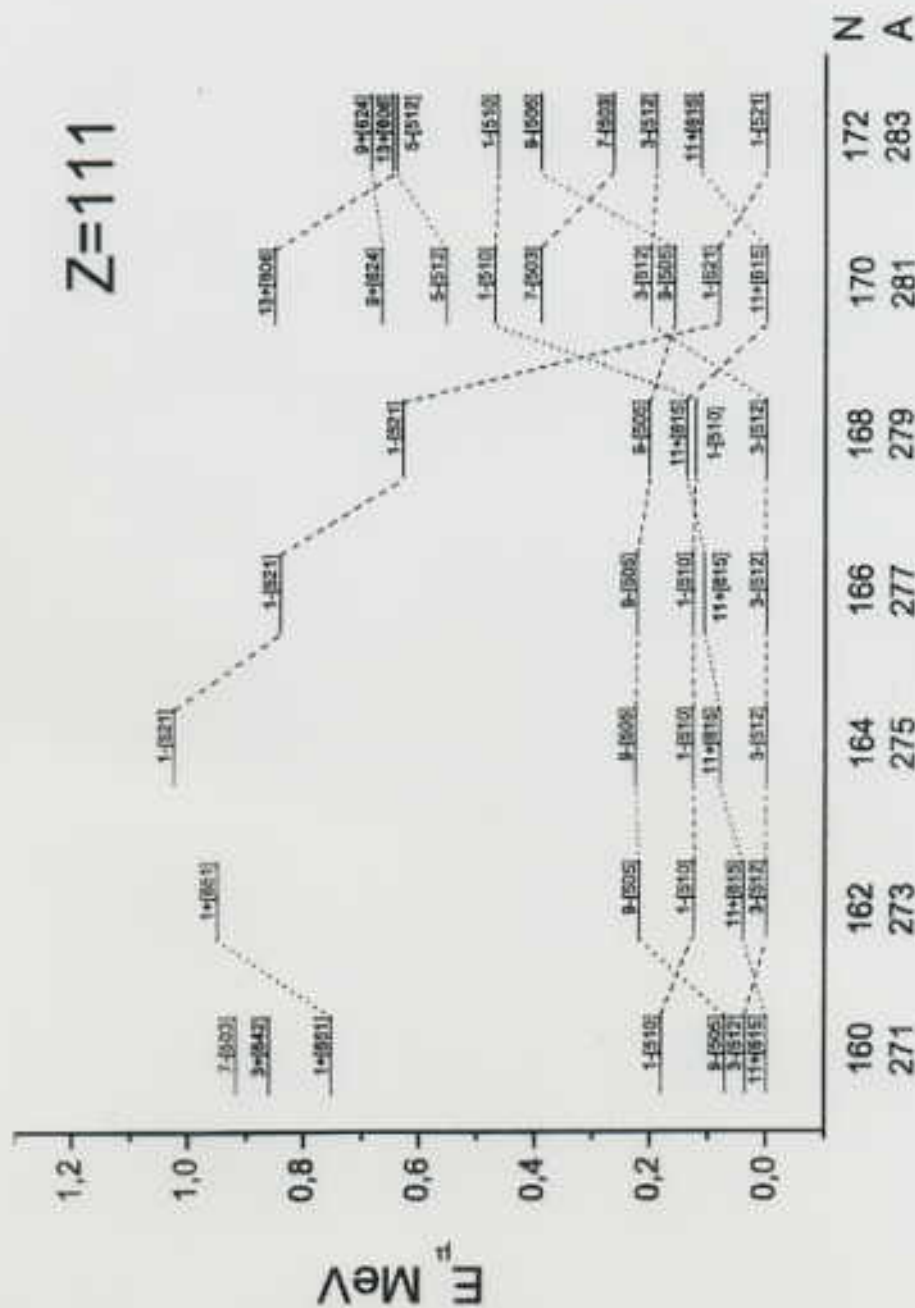


Fig. 12. Same as in Fig. 3, but for the element 111.

$\tilde{Z} [512]$ pseudo-spin doublet $\tilde{\Lambda} = 1$

$\tilde{Z} [510]$

neutron analog: ^{187}Os